NAVAL POSTGRADUATE SCHOOL
Monterey, California

THESIS

HOPF BIFURCATIONS IN PATH CONTROL OF MARINE VEHICLES

by

Zeki Okan Oral

June, 1993

Thesis Advisor: Fotis A. Papoulias

Approved for public release; distribution is unlimited.

UNCLASSIFIED

SECURITY CLASSIFICATION OF THIS PAGE

REPORT DOCUMENTATION PAGE

1a. REPORT SECURITY CLASSIFICATION: UNCLASSIFIED	1b. RESTRICTIVE MARKINGS
2a. SECURITY CLASSIFICATION AUTHORITY	3. DISTRIBUTION/AVAILABILITY OF REPORT: Approved for public release; distribution is unlimited
2b. DECLASSIFICATION/DOWNGRADING SCHEDULE	
4. PERFORMING ORGANIZATION REPORT NUMBER(S)	5. MONITORING ORGANIZATION REPORT NUMBER(S)
6a. NAME OF PERFORMING ORGANIZATION: Naval Postgraduate School; 6b. OFFICE SYMBOL (if applicable): ME	7a. NAME OF MONITORING ORGANIZATION: Naval Postgraduate School
6c. ADDRESS (City, State, and ZIP Code): Monterey, CA 93943-5000	7b. ADDRESS (City, State, and ZIP Code): Monterey, CA 93943-5000
8a. NAME OF FUNDING/SPONSORING ORGANIZATION; 8b. OFFICE SYMBOL (if applicable)	9. PROCUREMENT INSTRUMENT IDENTIFICATION NUMBER
8c. ADDRESS (City, State, and ZIP Code)	10. SOURCE OF FUNDING NUMBERS: PROGRAM ELEMENT NO. / PROJECT NO. / TASK NO. / WORK UNIT ACCESSION NO.

11. TITLE (Include Security Classification)
HOPF BIFURCATIONS IN PATH CONTROL OF MARINE VEHICLES

12. PERSONAL AUTHOR(S)
Zeki Okan Oral

13a. TYPE OF REPORT	13b. TIME COVERED	14. DATE OF REPORT (Year, Month, Day)	15. PAGE COUNT
Master's Thesis	FROM 09/92 TO 06/93	June 1993	76

16. SUPPLEMENTARY NOTATION The views expressed in this thesis are those of the author and do not reflect the official policy or position of the Department of Defense or the United States Government.

17. COSATI CODES		
FIELD	GROUP	SUB-GROUP

18. SUBJECT TERMS (Continue on reverse if necessary and identify by block number)
Hopf bifurcation, Supercritical, Subcritical, Center Manifold Theorem, Limit Cycle, Periodic Solutions, Marine Vehicle Control.

19. ABSTRACT (Continue on reverse if necessary and identify by block number)

The problem of loss of stability of marine vehicles under cross track error control in the presence of mathematical versus actual system mismatch is analyzed. Emphasis is placed on studying the response of the system after initial loss of stability of straight line motion. Center manifold reduction and integral averaging techniques are used in order to study the bifurcations to periodic solutions and stability of the resulting limit cycles. Numerical integrations are utilized to confirm the theoretical results and to establish regions of asymptotic stability. The methods used in this work demonstrate the significance of nonlinear terms in assessing the final response of the system.

20. DISTRIBUTION/AVAILABILITY OF ABSTRACT	21. ABSTRACT SECURITY CLASSIFICATION
[X] UNCLASSIFIED/UNLIMITED [ ] SAME AS RPT. [ ] DTIC USERS	UNCLASSIFIED
22a. NAME OF RESPONSIBLE INDIVIDUAL: Fotis A. Papoulias	22b. TELEPHONE (Include Area Code): (408) 656-3381 / 22c. OFFICE SYMBOL: ME/PA

DD FORM 1473, 84 MAR — 83 APR edition may be used until exhausted. All other editions are obsolete.

SECURITY CLASSIFICATION OF THIS PAGE

UNCLASSIFIED

Approved for public release; distribution is unlimited.

Hopf Bifurcations in Path Control of Marine Vehicles

by

Zeki Okan Oral
Lieutenant J. G., Turkish Navy
B.S., Turkish Naval Academy, 1987

Submitted in partial fulfillment
of the requirements for the degree of

MASTER OF SCIENCE IN MECHANICAL ENGINEERING

from the

NAVAL POSTGRADUATE SCHOOL
June 1993

Author: 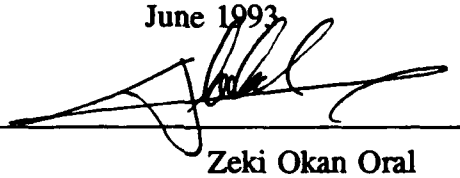
Zeki Okan Oral

Approved by: 
Fotis A. Papoulias, Thesis Advisor

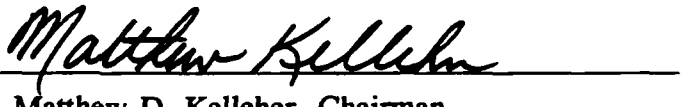
Matthew D. Kelleher, Chairman
Department of Mechanical Engineering

ABSTRACT

The problem of loss of stability of marine vehicles under cross track error control in the presence of mathematical versus actual system mismatch is analyzed. Emphasis is placed on studying the response of the system after initial loss of stability of straight line motion. Center manifold reduction and integral averaging techniques are used in order to study the bifurcations to periodic solutions and stability of the resulting limit cycles. Numerical integrations are utilized to confirm the theoretical results and to establish regions of asymptotic stability. The methods used in this work demonstrate the significance of nonlinear terms in assessing the final response of the system.

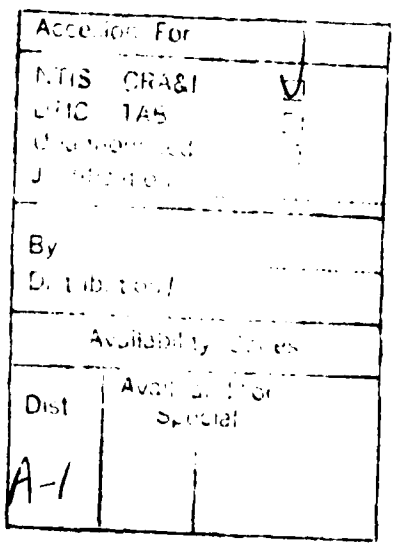

TABLE OF CONTENTS

TABLE OF SYMBOLS

a	dummy independent variable, or yaw rate coefficient in Nomoto's model
a_1	equivalent spring restoring moment coefficient
a_3	slowing down effect of rudder
A	linearized system matrix
b	rudder angle in Nomoto's model
c	parameter for variance of gain and hydrodynamic coefficients
c_{crit}	bifurcation valu of c
C_D	drag coefficient
I_z	vehicle mass moment of inertia
K	cubic stability coefficient
K_ψ, K_r, K_y	controller gains
m	vehicle mass
N	yaw moment
N_a	derivative of N with respect to a
PAH	Poincare´-Andronov-Hopf Bifurcation
r	yaw rate
R	polar coordinate of transformed reduced system
T	matrix of eigenvectors of A, or limit cycle period
v	sway velocity

X	state variables vector
x_G	body fixed coordinate of vehicle center of gravity
y	deviation off the commanded path
Y	sway force
Y_a	derivative of Y with respect to a
z	stable varibles vector vector in canonical form
z_1, z_2	critical variables of z
z_3	stable coordinate of z
α_0, α_1, α_2	coefficients of desired characteristic equation
β	real part of critical pair of eigenvalues
β'	derivative of β with respect to c evaluated at c_{crit}
δ	rudder angle control law
δ_0	linearized rudder angle control law
δ_{sat}	saturation limit of rudder angle
ϵ	critical difference $c - c_{crit}$
θ	polar coordinate of transformed reduced system
ψ	vehicle headind angle
ω_n	natural frequency
ω	imaginary part of critical pair of eigenvalues
ω'	derivative of ω with respect to c evaluated at c_{crit}

ACKNOWLEDGMENT

I wish to thank my thesis advisor Professor Fotis A. Papoulias for his guidance, and encouragement in this research.

I. INTRODUCTION

Accurate path control of ships and underwater vehicles along prescribed geographical paths is a fundamental problem which is becoming increasingly important, particularly as the missions of ocean vehicles become more sophisticated with strict requirements for performance. In order for a control law to be able to perform its mission in a realistic operational scenario it has to be robust enough so that it can maintain stability and accuracy of operations in the presence of modeling errors and environmental uncertainties. The robustness properties of the design are particularly important due to the unpredictable nature of the ocean environment and the changes in the hydrodynamic characteristics of the vehicle during turning, changes in the forward speed, or operations in proximity to other objects in the area. For these reasons, there exists a need for the analysis of the robustness characteristics of a particular control law design and the establishment of a rational operational envelope based on stability and performance criteria. Previous studies (Parsons & Cuong, 1977) showed that gain adaptation is highly desirable due to changes in the linearized vehicle hydrodynamics with different operating conditions, such as depth under keel. The resulting adaptation scheme (Parsons & Cuong, 1980) required significant vehicle motion which may be undesirable when operating in restricted water, or in object recognition and localization tasks. Integral control techniques (Parsons & Cuong, 1981) proved quite effective, but neglected the behavior of the vehicle which becomes very important at low speeds and

hover operations. Model based compensators exhibit robust behavior under conditions of parameter uncertainty which is as good as the classical linear quadratic regulators for linear output feedback systems (Healey, 1992). Alternatively, sliding mode controllers exhibit very robust characteristics given an estimate of the parameter uncertainty and/or disturbances (Papoulias & Healey, 1992), (Yoeger & Slotine, 1985). Sliding mode control, however, does not offer an infinitely robust design, and it suffers from a series of bifurcation phenomena and loss of stability unless proper care is exercised (Papoulias, 1991).

In this work we analyze the problem of loss of stability of a path keeping control law under conditions far from nominal. We assume that the autopilot has been designed based on a nominal model, whereas the actual system is different. For demonstration purposes we employ a linear full state feedback control law, but the methods are quite general and can be used for other designs as well. The main loss of stability cases analyzed here occur in the form of generic bifurcations to periodic solutions (Guckenheimer & Holmes, 1983). We use center manifold reduction techniques and averaging in order to capture the stability properties of the resulting limit cycles (Chow & Mallet-Paret, 1977). Particular emphasis is placed on the control gains as the primary bifurcation parameters, since they are related to gain margins in linear control theory (Friedland, 1986). We make extensive use of numerical integrations in order to confirm the theoretical results. All computations in this work are conducted for the NPS autonomous underwater vehicle (Bahrke, 1992), and all results are presented in standard

dimensionless quantities with respect to vehicle length, 7.3 ft, and nominal forward speed, 2 ft/sec.

II. PROBLEM FORMULATION

A. INTRODUCTION

The equations of motion of an ocean vehicle in the horizontal plane are presented in this chapter. A linear feedback control law is designed based on the linearized equations in yaw, sway, and rate of change of heading angle and lateral deviation error to provide path keeping. Loss of stability is examined for small changes from nominal in feedback gains, and system properties.

B. EQUATIONS OF MOTION

The mathematical modeling of a steering system of a vehicle consists of the nonlinear sway and yaw equations of motion. Newton's equations of motion in a moving coordinate frame fixed at the ships geometrical center are[1]

$$m(\dot{v}+r+x_G\dot{r}) = Y_{\dot{r}}\dot{r}+Y_{\dot{v}}\dot{v}+Y_r r+Y_v v+Y_{\delta_s}\delta_s+Y_{\delta_b}\delta_b - \int_{bow}^{stern} C_D h(\zeta)(v+\zeta r)\,|v+\zeta r|\,d\zeta \tag{1}$$

$$I_z\dot{r}+mx_G(\dot{v}+r) = N_{\dot{r}}+N_{\dot{v}}\dot{v}+N_r r+N_v v+N_{\delta_s}\delta_s+N_{\delta_b}\delta_b - \int_{stern}^{bow} C_D h(\zeta)(v+\zeta r)\,|v+\zeta r|\,d\zeta \tag{2}$$

[1] Equations are nondimensionalized with constant forward speed u,ship length L, and the dimensionless time being t.u/L.

where only nonzero terms are kept in the model and the symbols are explained in the nomenclature. The cross flow integral drag terms in the equations of motion are very important in low speeds, but for higher speeds their effect is much smaller and the steering response predominantly linear. Also for maximum maneuverability, the vehicle bow rudder is deflected at the same amount and opposite to the stern rudder.

Equations (1), and (2) can be written in the form

$$\dot{v}=a_{11}v+a_{12}r+b_1\delta \tag{3}$$

$$\dot{r}=a_{21}v+a_{22}r+b_2\delta \tag{4}$$

where

$$\begin{aligned}
Da_{11} &= (I_z-N_{\dot{r}})Y_{\dot{v}}-(mx_G-Y_{\dot{r}})N_{\dot{v}} \quad , \\
Da_{12} &= (I_z-N_{\dot{r}})(m-Y_{\dot{r}})-(mx_G-y_{\dot{r}})(n_{\dot{r}}-mx_G) \quad , \\
Da_{21} &= (m-Y_{\dot{v}})N_{\dot{v}}-(mx_G-N_{\dot{v}})Y_{\dot{v}} \quad , \\
Da_{22} &= (m-Y_{\dot{v}})(N_{\dot{r}}-mx_G)-(mx_G-N_{\dot{v}})(Y_{\dot{r}}-m), \\
Db_1 &= (I_{zN_{\dot{r}}})(Y_{\delta_s}-Y_{\delta_p})-(mx_G-Y_{\dot{r}})(N_{\delta_s}-N_{\delta_p}) \quad , \\
Db_2 &= (m-Y_{\dot{v}})(N_{\delta_s}-N_{\delta_p}) \quad , \\
D &= (I_z-N_{\dot{r}})(m-Y_{\dot{v}})-(mx_G-Y_{\dot{r}})(N_{\dot{r}}-mx_G)
\end{aligned} \tag{5}$$

The transfer function between rudder angle δ and yaw angular velocity r is obtained from Equations (3) and (4).

$$\frac{r}{\delta} = \frac{b_2S+(a_{21}b_1-a_{11}b_2)}{S^2-(a_{11}+a_{22})S+(a_{11}a_{22}-a_{12}a_{21})} \tag{6}$$

For low frequency maneuvering motions this second order equation can be approximated by expanding in Taylor series and keeping only the first order terms only

$$\frac{r}{\delta} = \frac{b}{s-a} \quad or \quad \dot{r} = ar + b\delta \tag{7}$$

where

$$a = \frac{(a_{11}a_{22} - a_{12}a_{21})(a + 21bl - a_{11}b_2)}{(a_{11} + a_{22})(a_{21}b_1 - a_{11}b_2) + b_2(a_{11}a_{22} - a_{12}a_{21})}$$

$$b = \frac{(a_{21}b_1 - a_{11}b_1)^2}{(a_{11} + a_{22})(a_{21}b_1 - a_{11}b_1 - a_{11}b_2) + b_2(a_{11}a_{22} - a_{12}a_{21})} \tag{8}$$

Equation (7), Nomoto's Equation is very useful in control system design since no sway velocity feedback necessary, and it gives the fundamental turning performance. At steady state, Equation (6) turns out to be

$$\begin{aligned} \dot{r} &= 0 \\ ar + b\delta &= 0 \\ r &= \frac{b}{a}\delta \end{aligned} \tag{9}$$

From Equation (9) it can be seen that the relationship between yaw rate and rudder control angle are linear with a slope -b/a. Experimental results show that the actual relationship is not linear. Large increases in rudder angle fail to increase the yaw rate according to the amount predicted from Equation (9).

The linear change in the time derivative of yaw rate due to rudder angle can be augmented by a nonlinear term of the form 'a_3r^3'. This is introduced to model the appropriate speed loss during turning. The term 'a_3' has the same sign as 'a'. The new yaw equation is therefore

$$\dot{r}=ar+a_3r^3+b\delta \tag{10}$$

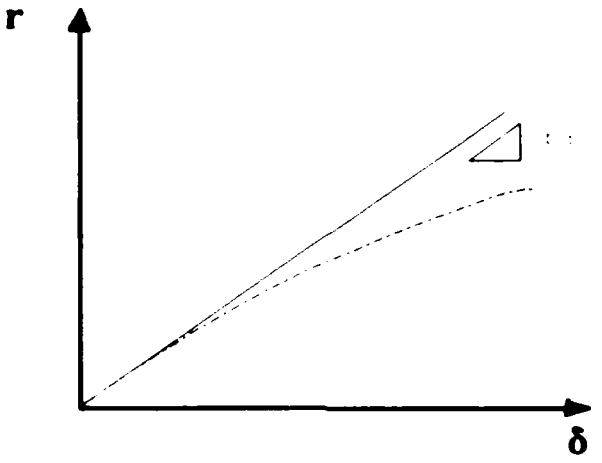

Figure 1 *Difference* between Nomoto's equations and experimental results.

The model becomes complete with the expression of yaw rate and the inertial deviation rate from the commanded path. Therefore the coupled nonlinear equations of motion for the marine vehicle in the horizontal plane are

$$\dot{\psi} = r \tag{11}$$

$$\dot{r} = ar+a_3r^3+b\delta \tag{12}$$

$$\dot{y} = \sin\psi \tag{13}$$

This system of equations forms the basis for the controller design.

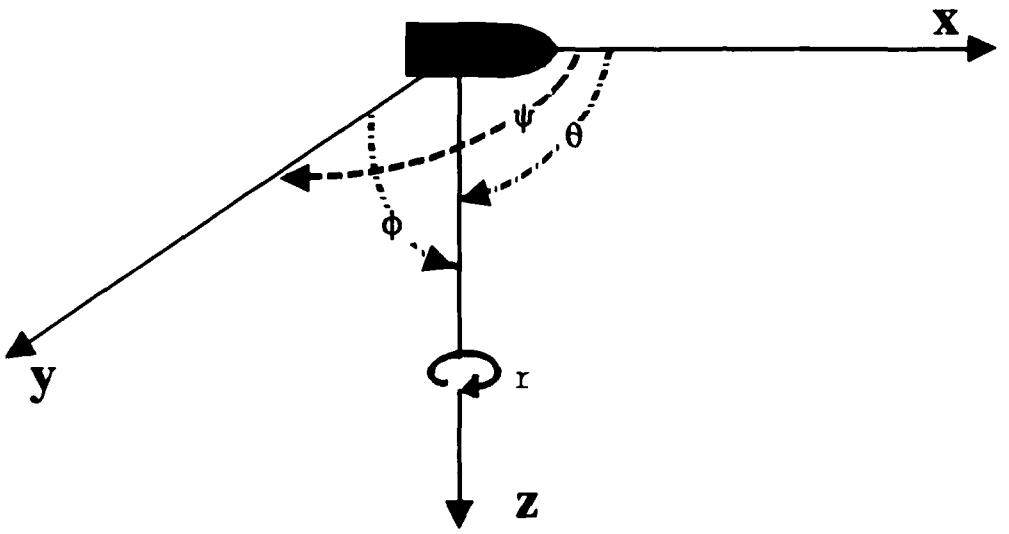

Figure 2

C. CONTROL LAW

Equations (11), (12), (13) govern the steering control of the model used in this section. The control law can be expressed as,

$$\delta = \delta_{sat} \tanh\left(\frac{\delta_0}{\delta_{sat}}\right) \qquad (14)$$

where in the vicinity of $\psi = r = y = 0$ we have

$$\delta_0 = K_\psi \psi + K_r r + K_y y \tag{15}$$

δ is the rudder angle and K_ψ ,K_r , K_y are the control gains of the system. The linear control law is δ_0 . The rudder angle δ is defined by a hyperbolic tangent function to include the saturation to our problem as shown in Figure (3). Saturation occurs at δ_{sat} which is the saturation limit generally can be taken as 0.4 rad. The linearized form of equation of motions in the vicinity of $\psi = r = y = 0$ are

$$\dot{\psi} = r \tag{16}$$

$$\dot{r} = ar + b\delta_0 \tag{17}$$

$$\dot{y} = \psi \tag{18}$$

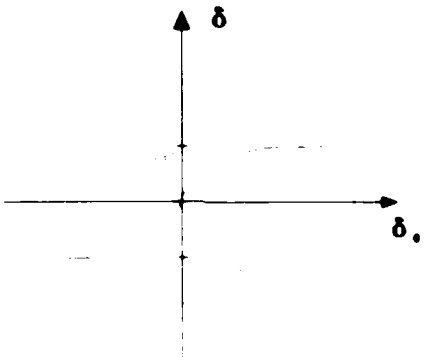

Figure 3

These equations can be expressed in space state form as

$$\dot{X} = AX \tag{19}$$

A is the Jacobian matrix of the system and X is the state vector

$$A = \begin{bmatrix} 0 & 1 & 0 \\ bK_{\psi} & a+bK_r & bK_y \\ 1 & 0 & 0 \end{bmatrix} \tag{20}$$

$$X = [\ \psi,\ r,\ y\ ]^T \tag{21}$$

The characteristic equation of the matrix A is

$$\lambda^3-(a+bK_r)\lambda^2-bK_{\psi}\lambda-bK_y=0 \tag{22}$$

The desired characteristic equation has the form

$$\lambda^3+\alpha_2\lambda^2+\alpha_1\lambda+\alpha_0=0 \tag{23}$$

The gains can be generated in terms of the coefficient of actual and desired characteristic equation from Equations (22) and (23).

$$K_{\psi} = -\frac{\alpha_1}{b} \tag{24}$$

$$K_r = -\frac{\alpha_2-a}{b} \tag{25}$$

$$K_v = -\frac{\alpha_0}{b} \tag{26}$$

The desired characteristic equation can be written with respect to the desired natural frequency and some optimum coefficients. The ITAE criterion for a third order equation is (Dorf, 1992)

$$S^3 + 1.75\,\omega_n S^2 + 2.15\,\omega_n^2 S + \omega_n^3 = 0 \tag{27}$$

Therefore the control gains can be calculated for a given natural frequency, as

$$\begin{aligned} \alpha_0 &= \omega_n^3 \\ \alpha_1 &= 2.15\,\omega_n^2 \\ \alpha_2 &= 1.75\,\omega_n \end{aligned} \tag{28}$$

D. LOSS OF STABILITY

1. Introduction

The control law guarantees stability if all real parts of eigenvalues of the jacobian matrix are negative. Equation (23) is stable with the chosen control gains. A small perturbation in the control gains or coefficients of the system affects its stability. In this section we presented the computations for the critical value for change in the gains and the coefficients of the system.

2. Stability Considerations

For a system with a third order characteristic equation, the Routh Hurwitz criterion (Dorf, 1992) requires for stability

$$\alpha_2\,\alpha_1 \geq \alpha_0 \tag{29}$$

a. Perturbation in K_v

The change in K_v is defined by a coefficient **c**, where **c** is any real number. The linearized equations of the system for a small change in K_v are

$$\begin{aligned} \dot{\psi} &= r \\ \dot{r} &= ar + b\delta_0 \\ \dot{y} &= \psi \end{aligned} \tag{30}$$

where the control law is

$$\delta_0 = cK_\psi \psi + K_r r + K_y y \tag{31}$$

Therefore the characteristic equation is

$$\lambda^3 - (a + bK_r)\lambda^2 - cbK_\psi \lambda - bK_y = 0 \tag{32}$$

Equation (32) should meet the Routh Hurwitz criterion for stability.

$$(a + bK_r)cbK_\psi \geq -bK_y \tag{33}$$

The critical value of **c** where a stability change occurs in the system is presented in Equation (34)

$$c_{crit_{K_\psi}} = \frac{\alpha_0}{\alpha_1 \alpha_2} \tag{34}$$

Using the coefficients, the critical **c** is

$$c_{crit_{K_\psi}} = 0.2658 \tag{35}$$

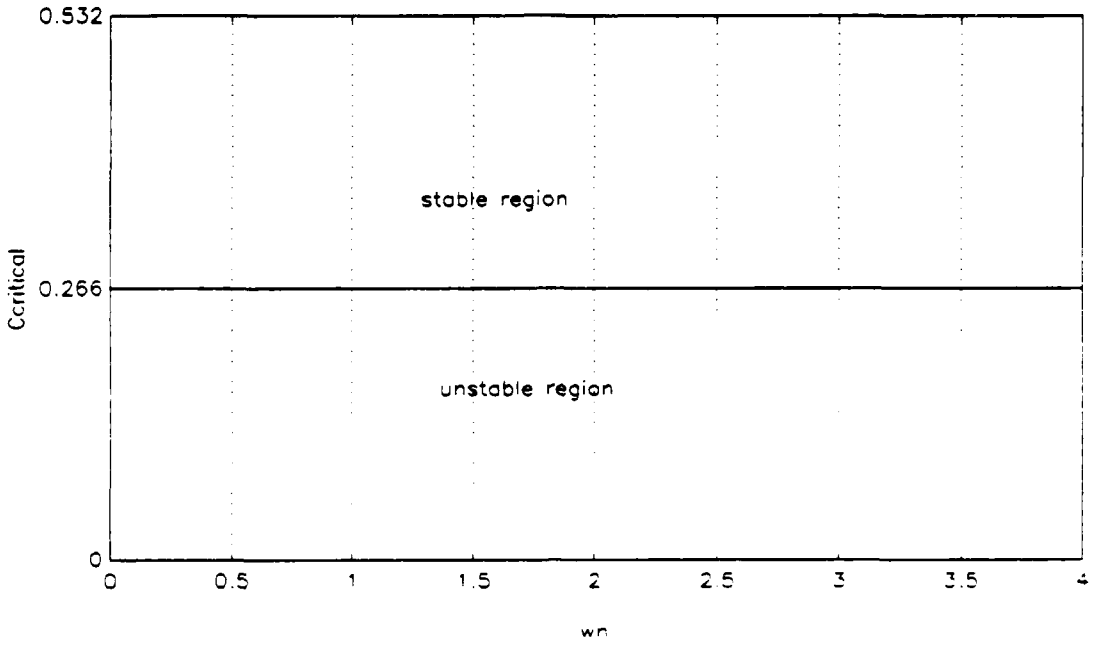

Figure 4 c_{crit} vs natural frequency for K_ψ.

b. Perturbation In K_r

Similarly for perturbation in K_r the characteristic equation is

$$\lambda^3 - (a + cbK_r)\lambda^2 - bK_\psi \lambda - bK_y = 0 \tag{36}$$

The critical value of **c**,

$$c_{crit_{K_r}} = \frac{\alpha_0 + \alpha_1 a}{\alpha_1(\alpha_2 + a)} \tag{37}$$

or

$$c_{crit_{K_r}} = \frac{\omega_n + 2.15a}{2.15(1.75\omega_n + a)} \tag{38}$$

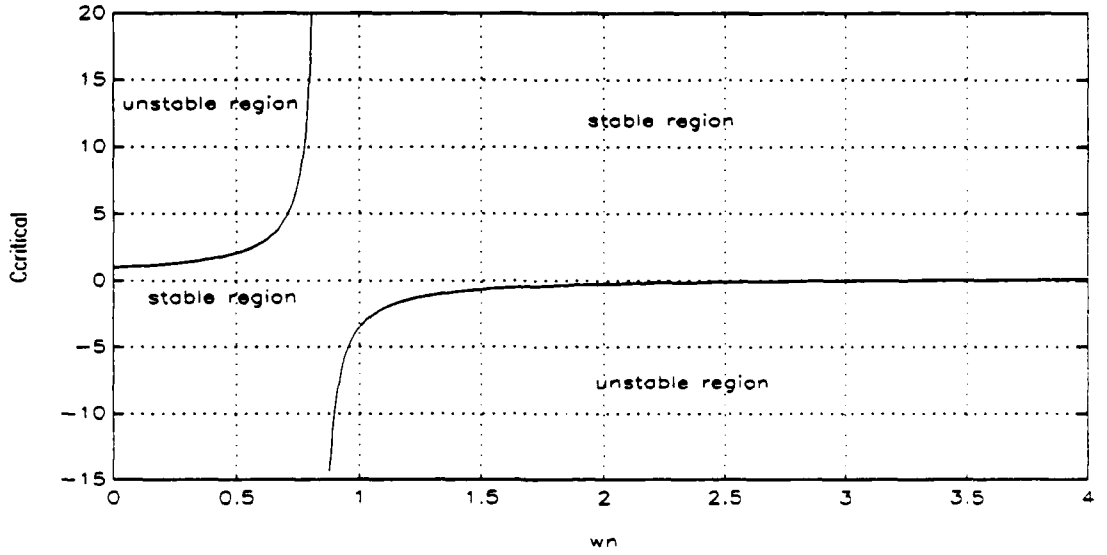

Figure 5 c_{crit} versus natural frequency for K_r.

c. Perturbation In K_y

The results for changes in K_y are presented similarly. The characteristic equation, is

$$\lambda^3 - (a + bK_r)\lambda^2 - bK_\psi \lambda - bcK_y = 0 \tag{39}$$

The critical value of **c** is

$$c_{crit_{K_y}} = \frac{\alpha_1 \alpha_2}{\alpha_0} \tag{40}$$

$$c_{crit_{K_y}} = 3.7625 \tag{41}$$

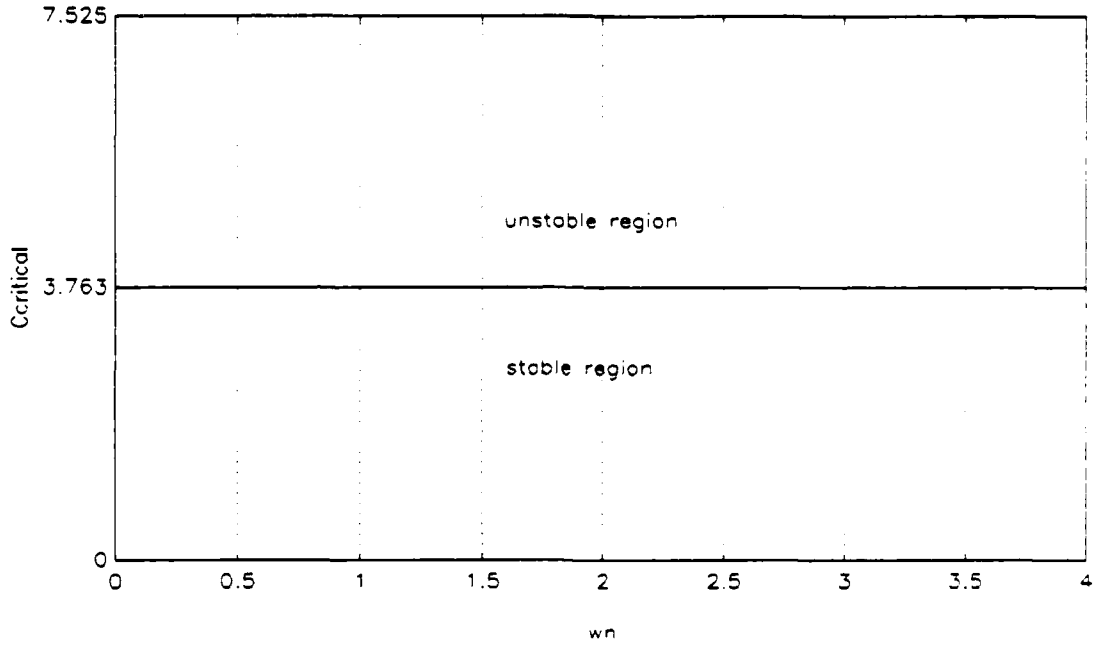

Figure 6 c_{crit} versus natural frequency for K_y.

d. Perturbation in a

After similar calculations the critical value of c is

$$c_{crit_a} = \frac{(\alpha_2 + a)\alpha_1 - \alpha_0}{a\alpha_1} \tag{42}$$

or

$$c_{crit_a} = \frac{1.28484\ \omega_n}{a} + 1 \tag{43}$$

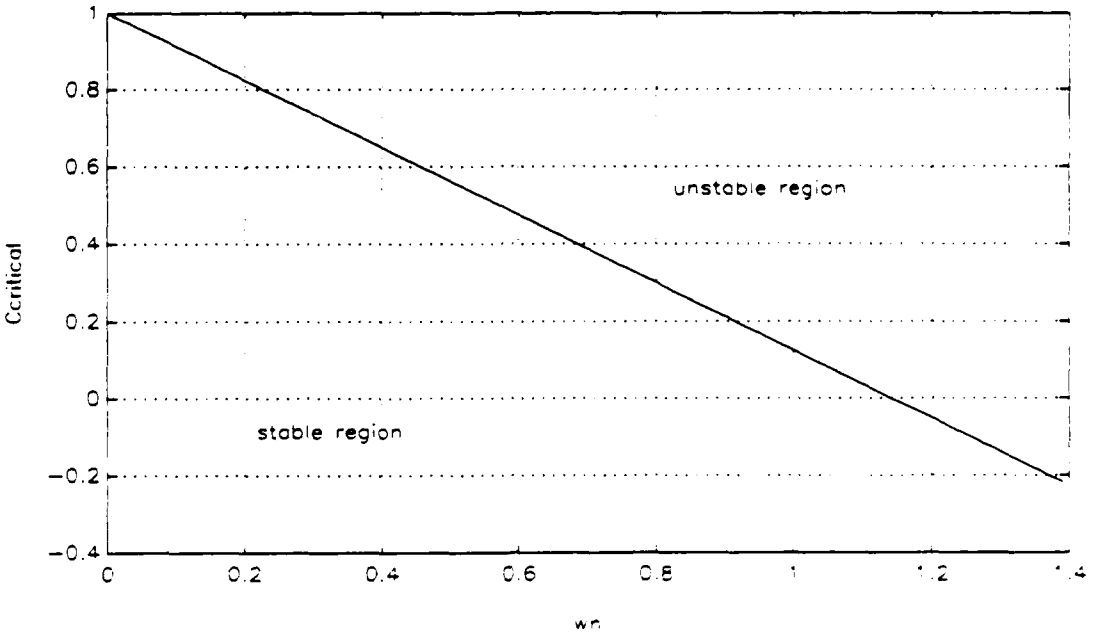

Figure 7 c_{crit} versus natural frequency for a

e. Perturbation in b

After similar calculations as with the other cases the characteristic equation is,

$$\lambda^3 + (c(\alpha_2 + a) - a)\alpha^2 - c\alpha_1\lambda + c\alpha_0 = 0 \tag{44}$$

and the critical values are

$$c_{crit_b} = \frac{\alpha_0 + a\ \alpha_1}{\alpha_1(\alpha_2 + a)} \tag{45}$$

or

$$c_{crit_b} = \frac{\omega_n + 2.15a}{2.15(1.75\,\omega_n + a)} \tag{46}$$

Examining Equation (46), we note that all the coefficients of polynomial must have the same sign, if all the roots are in the left hand plane.The necessary conditions for stability are,

$$\begin{aligned} c &\geq 0 \\ c(\alpha_2 + a) - a &\geq 0 \end{aligned} \tag{47}$$

The system is unstable for all values of the natural frequency if **c** is less then zero.When the natural frequency is in the interval $0 \leq \omega_n \leq |a/1.75|$ stability changes from stable to unstable with an increase in **c** (Figure (8)) for positive values of **c**. In the interval $\omega_n \geq |\mathbf{2.15a}|$ stability changes from unstable to stable while **c** crosses the critical point again for positive values of **c**. In both cases a pair of complex conjugate eigenvalues crosses the imaginary axis. Stability is also lost when **c** becomes negative, but this is associated with a real eigenvalue crossing zero. In this work we concentrate on the $\mathbf{c > 0}$ case since in applications it is unlikely that a change in the sign of **b** will occur.

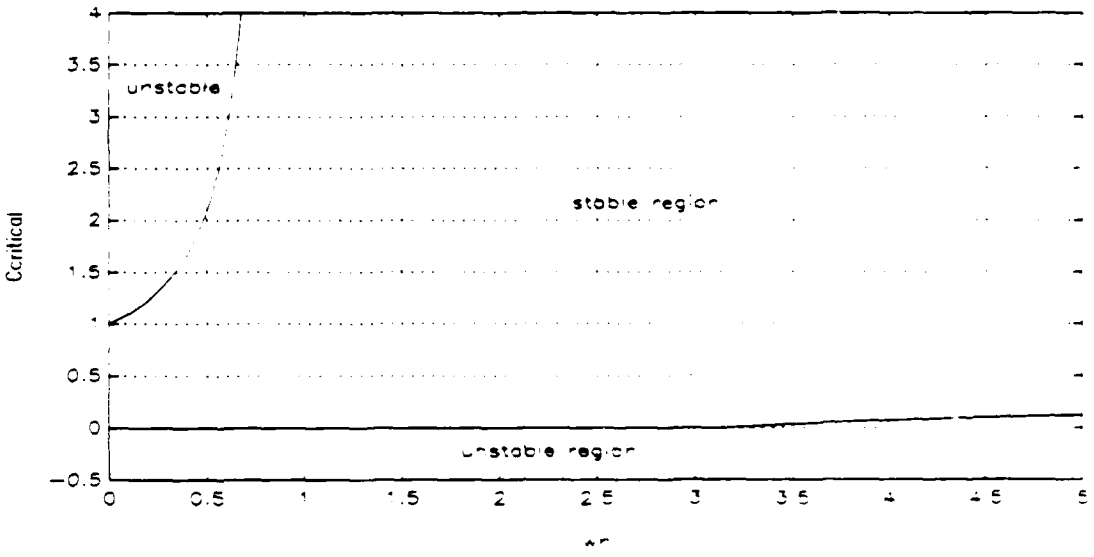

Figure 8 $\mathbf{c_{crit}}$ versus natural frequency for **b**. The $\mathbf{c_{crit}}$ goes to infinity asymptotically at $\omega_n = -a/1.75$.

III. HOPF BIFURCATION

A. INTRODUCTION

Hopf bifurcation is the simplest bifurcation, in which under the variation of a single control parameter a stable focus equilibrium bifurcates into an unstable focus surrounded by a growing limit cycle. As **c** crosses the critical value one pair of complex conjugate eigenvalues of the linear system matrix crosses transversely the imaginary axis. In this generic Poincare' - Andronov - Hopf bifurcation a family of periodic solutions coexists with the stable / unstable nominal equilibrium state. Locally as **c** approaches $\mathbf{c}_{crit}$ the periodic solutions are located on the two dimensional Euclidean plane spanned by the eigenvectors of Jacobian matrix of the system which corresponds to the critical pair of eigenvalues. In this chapter stability properties of the periodic solutions are established. In order to establish those properties the main nonlinear terms that dominate the system are isolated. Center manifold theory is used to reduce the flow to a two dimensional manifold. The method of averaging is applied to the reduced system. Hopf bifurcations are examined for small changes in each gain and system dynamics coefficients.

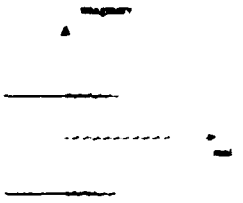

Figure 9

B. THIRD ORDER EXPANSION OF THE SYSTEM EQUATIONS

1. Perturbation in K_ψ

In this case the equations of motions are

$$\begin{aligned} \dot{\psi} &= r \\ \dot{r} &= ar + a_3 r^3 + b\delta \\ \dot{y} &= \sin\psi \end{aligned} \tag{48}$$

where

$$\begin{aligned} \delta &= \delta_{sat} \tanh\left(\frac{\delta_0}{\delta_{sat}}\right) \\ \delta_0 &= cK_\psi \psi + K_r r + K_y y \end{aligned} \tag{49}$$

The trivial equilibrium state is characterized by $\psi = r = y = 0$ .Taylor expansion of the nonlinear terms about the equilibrium gives

$$\begin{aligned} \sin\psi &= \psi - \frac{\psi^3}{3!} + O(5) \\ \delta &= \delta_0 - \frac{{\delta_0}^3}{3\delta_{sat}^2} + O(5) \end{aligned} \tag{50}$$

The system equations are

$$\begin{aligned} \dot{\psi} &= r \\ \dot{r} &= ar + a_3 r^3 + b\delta_0 - \frac{b\delta_0^3}{3\delta_{sat}^3} \\ \dot{y} &= \psi - \frac{\psi^3}{6} \end{aligned} \tag{51}$$

In state space form they are written as

$$\dot{X} = AX + g^3(X) \tag{52}$$

where A is the linearized system matrix, and $g^3(x)$ contains the nonlinear terms,

$$A = \begin{bmatrix} 0 & 1 & 0 \\ cbK_\psi & a + bK_r & bK_y \\ 1 & 0 & 0 \end{bmatrix} \tag{53}$$

$$\begin{aligned} g_1^3(x) &= 0 \\ g_2^3(x) &= -\frac{b}{3\delta_{sat}^2}\delta_0^3 \\ g_3^3(x) &= -\frac{\psi^3}{6} \end{aligned} \tag{54}$$

where the $\delta_0{}^3$ term is computed as

$$\begin{aligned} \delta_0^3 = {} & cK_\psi^3\psi^3 + K_r^3 r^3 + K_y^3 y^3 \\ & 3c^2K_\psi^2(K_r r + K_y y) + 3K_r^2 r^2(cK_\psi\psi + K_y y) \\ & 3K_y^2 y^2(cK_\psi\psi + K_r r) + 6cK_\psi K_r K_y \psi r y \end{aligned} \tag{55}$$

With the computed gains from equations (24), (25), (26), Jacobian matrix is

$$A = \begin{bmatrix} 0 & 1 & 0 \\ -c\alpha_1 & -\alpha_2 & -\alpha_0 \\ 1 & 0 & 0 \end{bmatrix} \tag{56}$$

The eigenvalues of matrix A are computed at the bifurcation point c_{cnt} from equation (34) where a pair of complex conjugate roots with real parts are obtained.

$$\lambda_1 = j\sqrt{\frac{\alpha_0}{\alpha_2}}$$

$$\lambda_2 = -j\sqrt{\frac{\alpha_0}{\alpha_2}} \qquad (57)$$

$$\lambda_3 = -\alpha_2$$

For the above system of equations a transformation matrix of eigenvectors can be introduced,

$$T = \begin{bmatrix} 1 & 0 & 1 \\ 0 & -\sqrt{\frac{\alpha_0}{\alpha_2}} & -\alpha_2 \\ 0 & \sqrt{\frac{\alpha_2}{\alpha_0}} & -1/\alpha_2 \end{bmatrix} \qquad (58)$$

The transformation

$$x = Tz \quad , \quad z = T^{-1}x \qquad (59)$$

transforms the system into its normal coordinate form,

$$\dot{z} = T^{-1}ATz + T^{-1}g^3(Tz) \qquad (60)$$

where,

$$T^{-1} = \begin{bmatrix} \left(\frac{\alpha_0}{\alpha_2}\right)^{3/2} \frac{1}{\alpha_2^3 + \alpha_0} & \sqrt{\frac{\alpha_2}{\alpha_0}} & \sqrt{\frac{\alpha_0}{\alpha_2}} \\ 0 & \frac{1}{\alpha_2} & \alpha_2 \\ 0 & \sqrt{\frac{\alpha_2}{\alpha_0}} & \sqrt{\frac{\alpha_0}{\alpha_2}} \end{bmatrix} \qquad (61)$$

and

$$T^{-1}AT = \begin{bmatrix} 0 & -\sqrt{\frac{\alpha_0}{\alpha_2}} & 0 \\ \sqrt{\frac{\alpha_0}{\alpha_2}} & 0 & 0 \\ 0 & 0 & \alpha_2 \end{bmatrix} \qquad (62)$$

The transformation of physical variables to normal coordinates is

$$\mathbf{x} = \mathbf{T}\,\mathbf{z}\ ,$$

$$\begin{aligned} \psi &= z_1 + z_3 \\ r &= \sqrt{\frac{\alpha_0}{\alpha_2}}\, z_2 - \alpha_2 z_3 \\ y &= \sqrt{\frac{\alpha_2}{\alpha_0}}\, z_2 + \frac{1}{\alpha_2} z_3 \end{aligned} \qquad (63)$$

$$\begin{bmatrix} \psi \\ r \\ y \end{bmatrix} = \begin{bmatrix} 1 & 0 & 1 \\ 0 & \sqrt{\frac{\alpha_0}{\alpha_2}} & -\alpha_2 \\ 0 & \sqrt{\alpha_2} & 1 \\ & \sqrt{\alpha_0} & \alpha_2 \end{bmatrix} \begin{bmatrix} z_1 \\ z_2 \\ z_3 \end{bmatrix} \qquad (64)$$

The coordinate z_3 corresponds to the eigenvalue λ_3 which is real and negative. λ_1, λ_2 denote the complex conjugate pair with zero real parts. At the critical point two distinct eigenspaces are spanned by the eigenvectors associated with the two sets of eigenvalues. These eigenspaces can be viewed as local approximations of the invariant manifolds the center and the stable manifold. The system exhibits its essential bifurcational behavior on the centre manifold associated with λ_1 and λ_2. Centre manifold theory reduces the flow to a two dimensional manifold (Hopf bifurcation). According to centre manifold theory the coordinate z_3 is expressed in terms of z_1 and z_2, but this expression is higher order. Equation (64) can be written as,

$$\begin{aligned} \psi &= z_1 \\ r &= -\sqrt{\frac{\alpha_0}{\alpha_2}}\, z_2 \\ y &= \sqrt{\frac{\alpha_2}{\alpha_0}}\, z_2 \end{aligned} \qquad (65)$$

Substituting the equations (65) to (60) the system equations in normal coordinates become

$$\dot{z}_1 = -\sqrt{\frac{\alpha_0}{\alpha_2}}\, z_2 + r_{11} z_1^3 + r_{12} z_1^2 z_2 + r_{13} z_1 z_2^2 + r_{14} z_2^3$$
$$\dot{z}_2 = \sqrt{\frac{\alpha_0}{\alpha_2}}\, z_1 + r_{21} z_1^3 + r_{22} z_1^2 z_2 + r_{23} z_1 z_2^2 + r_{24} z_2^3 \qquad \textbf{(66)}$$

The terms $\mathbf{r}_{ij}$ are computed later from our equations at the bifurcation point $\mathbf{c}_{crit}$. For values of $\mathbf{c}$ in the neighborhood of the critical point, equation (66) becomes,

$$\dot{z}_1 = \beta' \epsilon z_1 - \left(\omega' \epsilon - \sqrt{\frac{\alpha_0}{\alpha_2}}\right) z_2 + r_{11} z_1^3 + r_{12} z_1^2 z_2 + r_{13} z_1 z_2^2 + r_{14} z_2^3$$
$$\dot{z}_2 = \left(\omega' \epsilon + \sqrt{\frac{\alpha_0}{\alpha_2}}\right) z_1 + \beta' \epsilon z_2 + r_{21} z_1^3 + r_{22} z_1^2 z_2 + r_{23} z_1 z_2^2 + r_{24} z_2^3 \qquad \textbf{(67)}$$

The parameter ϵ is the difference between $\mathbf{c}_{crit}$ and $\mathbf{c}$ or, $\mathbf{c} = \mathbf{c}_{crit} + \epsilon$. The terms β' and ω' are the derivative of the real and imaginary parts of eigenvalues with respect to $\mathbf{c}$ evaluated at $\mathbf{c} = \mathbf{c}_{crit}$, and computed from a perturbation series approach. The perturbation is expressed as follows from equation (34),

$$c = \frac{\alpha_0}{\alpha_1 \alpha_2} + \epsilon \qquad \textbf{(68)}$$

The characteristic equation can be written as follows for a small change for K_v in the neighborhood of $\mathbf{c}_{crit}$.

$$\lambda^3 + \alpha_2 \lambda^2 + \left(\frac{\alpha_0}{\alpha_2} + \alpha_1 \epsilon\right) \lambda + \alpha_0 = 0 \qquad \textbf{(69)}$$

The solutions of equation (69) are presented in equation (70)

$$\lambda_{1,2} = b_1 \epsilon \mp j\left(\sqrt{\frac{\alpha_0}{\alpha_2}} + c_1 \epsilon\right)$$
$$\lambda_3 = -\alpha_2 + a_1 \epsilon \tag{70}$$

The variables b_1 and c_1 can be found by substituting equation (70) to (69) and neglecting the successive powers ϵ^2, ϵ^3.

$$b_1 = -\frac{\alpha_2^2 \alpha_1}{2(\alpha_0 + \alpha_2^3)}$$
$$c_1 = \frac{\alpha_2 \alpha_1 \sqrt{\frac{\alpha_0}{\alpha_2}}}{2(\alpha_0 + \alpha_2^3)} \tag{71}$$

β' and ω' can be expressed by the definition of the derivative where ϵ is zero in the limit.

$$\beta' = \frac{b_1 \epsilon - 0}{\epsilon} = b_1$$
$$\omega' = \frac{\left(\sqrt{\frac{\alpha_0}{\alpha_2}} + c_1 \epsilon\right) - \sqrt{\frac{\alpha_0}{\alpha_2}}}{\epsilon} = c_1 \tag{72}$$

Equation (72) can be written in terms of the desired natural frequency,

$$\beta' = -0.6841\,\omega_n$$
$$\omega' = 0.5171\,\omega_n \tag{73}$$

a. Calculations of r_{IJ} Terms

The terms r_{ij} are generated by the last term of equation (60), where $T^{-1}g^3(Tz)$ is the third order nonlinear part. From equations (61) and (54)

$$T^{-1}g^3(Tz)=\frac{\alpha_2^{3/2}(\alpha_2^3+\alpha_0)}{\alpha_2^{3/2}}\begin{bmatrix}\frac{\alpha_0^{3/2}}{\alpha_2^{3/2}(\alpha_2^3+\alpha_0)} & \sqrt{\frac{\alpha_2}{\alpha_0}} & \sqrt{\frac{\alpha_0}{\alpha_2}}\\ 0 & -\frac{1}{\alpha_2} & \alpha_2\\ 0 & -\sqrt{\frac{\alpha_2}{\alpha_0}} & \sqrt{\frac{\alpha_0}{\alpha_2}}\end{bmatrix}\begin{bmatrix}0\\ -a_3\left(\frac{\alpha_0}{\alpha_2}\right)^{3/2}z_2^3-\frac{b}{\delta_{sat}^2}\delta_0^3\\ -\frac{1}{6}z_1^3\end{bmatrix} \tag{74}$$

where,

$$\delta_0^3 = \frac{1}{b^3}\left\{-\left(\frac{\alpha_0}{\alpha_2}\right)^3 z_1^3+3\left(\frac{\alpha_0}{\alpha_2}\right)^{5/2} a z_1^2 z_2-3\left(\frac{\alpha_0}{\alpha_2}\right)^2 a^2 z_1 z_2^2+a^3\left(\frac{\alpha_0}{\alpha_2}\right)^{3/2} z_2^3\right\} \tag{75}$$

After expanding the first row of equation (74) and organizing the terms, we get

$$r_{11} = \frac{\alpha_2}{\alpha_0}(\alpha_2^3+\alpha_0)\left(\frac{1}{3b^2\delta_{sat}^2}\left(\frac{\alpha_0}{\alpha_2}\right)^2-\frac{1}{6}\right) \tag{76}$$

$$r_{12} = -\left(\frac{\alpha_0}{\alpha_2}\right)^{1/2}(\alpha_2^3+\alpha_0)\frac{a}{b^2\delta_{sat}^2} \tag{77}$$

$$r_{13} = (\alpha_2^3+\alpha_0)\frac{a^2}{b^2\delta^{2}_{sat}} \tag{78}$$

$$r_{14} = -\left(\frac{\alpha_2}{\alpha_0}\right)(\alpha_2^3+\alpha_0)(a_3+\frac{a^3}{3b^2\delta_{sat}^2}) \tag{79}$$

Similarly after expanding the second row of equation (74) and organizing, we get

$$r_{21} = -(\alpha_2^3+\alpha_0)\{\frac{1}{3b^2\delta_{sat}^2}\frac{\alpha_0^{3/2}}{\alpha_2^{5/2}}+\frac{1}{6}\frac{\alpha_2^{5/2}}{\alpha_0^{3/2}}\} \tag{80}$$

$$r_{22} = \frac{\alpha_0}{\alpha_2^2}(\alpha_2^3+\alpha_0)\frac{a}{b^2\delta_{sat}^2} \tag{81}$$

$$r_{23} = -\frac{\alpha_0^{1/2}}{\alpha_2^{3/2}}(\alpha_2^3+\alpha_0)\frac{a^2}{b^2\delta_{sat}^2} \tag{82}$$

$$r_{24} = \frac{\alpha_2^3+\alpha_0}{\alpha_2}(a_3+\frac{a^3}{3b^2\delta_{sat}^2}) \tag{83}$$

b. Averaging

Equation (67) can be written in a simpler form .

$$\begin{aligned} \dot{z}_1 &= \beta'\epsilon z_1 - \left(\omega'\epsilon + \sqrt{\frac{\alpha_0}{\alpha_2}}\right) z_2 + F_1(z_1, z_2) \\ \dot{z}_2 &= \left(\omega'\epsilon + \sqrt{\frac{\alpha_0}{\alpha_2}}\right) z_1 + \beta'\epsilon z_2 + F_2(z_1, z_2) \end{aligned} \tag{84}$$

where F_1 and F_2 contain the third order expansion terms. The use of polar coordinates makes it possible to decouple equation (84) . We use the polar transformation

$$z_1 = R\cos(\theta) \quad , \quad z_2 = R\sin(\theta)$$

After some algebra, equation (83) can be expressed in terms of R and θ.

$$\dot{R} = \beta'\epsilon R + F_1(R\cos(\theta), R\sin(\theta))\cos(\theta) + F_2(R\cos(\theta), R\sin(\theta))\sin(\theta) \tag{85}$$

$$R\dot{\theta} = \left(\sqrt{\frac{\alpha_0}{\alpha_2}} + \omega'\epsilon\right) R + F_2(R\cos(\theta), R\sin(\theta))\cos(\theta) - F_1(R\cos(\theta), R\sin(\theta))\sin(\theta) \tag{86}$$

Equation (85) can be written as follows,

$$\dot{R} = \beta'\epsilon R + P(\theta) R^3 \tag{87}$$

where $P(\theta)$ is 2π periodic in the angular coordinate θ.

$$\begin{aligned} P(\theta) = {} & r_{11}\cos^4(\theta) + r_{12}\cos^3(\theta)\sin(\theta) + r_{13}\cos^2(\theta)\sin^2(\theta) + r_{14}\cos(\theta)\sin^3(\theta) \\ & + r_{21}\cos^3(\theta)\sin(\theta) + r_{22}\cos^2(\theta)\sin^2(\theta) + r_{23}\cos(\theta)\sin^3(\theta) + r_{24}\sin^4(\theta) \end{aligned} \tag{88}$$

Equation (87) is averaged over one cycle to obtain an equation with constant coefficients.

$$\dot{R} = \beta' \epsilon R + \mathrm{K} R^3 \tag{89}$$

where **K** is defined by,

$$\mathrm{K} = \frac{1}{2\pi} \int_0^{2\pi} P(\theta) d\theta \tag{90}$$

Equation (90) is simplified as equation (91) after evaluation of the integral.

$$\mathrm{K} = \frac{1}{8} [3 r_{11} + r_{13} + r_{22} + 3 r_{24}] \tag{91}$$

Equation (91) can be expressed in terms of the natural frequency,

$$\mathrm{K} = 0.452 [3 a_3 \omega_n^2 + \frac{\omega_n^2}{b^2 \delta_{sat}^2} (\omega_n^3 + \frac{a}{1.75} \omega_n + a^3) - \frac{1.75^2}{2} \omega_n] \tag{92}$$

Equation (87) can be expressed as,

$$\dot{\theta} = \sqrt{\frac{\alpha_0}{\alpha_2}} + \omega' \epsilon + F(\theta) R^2 \tag{93}$$

where,

$$\begin{aligned} F(\theta) = {} & r_{21} \cos^4(\theta) + r_{22} \cos^3(\theta) \sin(\theta) + r_{23} \cos^2(\theta) \sin^2(\theta) + r_{24} \cos(\theta) \sin^3(\theta) \\ & - r_{11} \cos^3(\theta) \sin(\theta) - r_{12} \cos^2(\theta) \sin^2(\theta) - r_{13} \cos(\theta) \sin^3(\theta) - r_{14} \sin^4(\theta) \end{aligned} \tag{94}$$

After averaging equation (93), a constant coefficient M is formed,

$$\dot{\theta} = \sqrt{\frac{\alpha_0}{\alpha_2} + \omega' \epsilon + MR^2} \tag{95}$$

where M is defined by,

$$M = \frac{1}{2\pi} \int_0^{2\pi} F(\theta) d\theta \tag{96}$$

or in terms of natural frequency,

$$M = 0.7949\,\omega_n^3 [\frac{3.9686}{\omega_n} - \frac{2.0256}{\omega_n} + \frac{1}{b^2 \delta_{sat}^2} \frac{1}{\sqrt{1.75}\omega_n^2} (1.75 a \omega_n - \frac{\omega_n^2}{1.75})(\frac{\omega_n^2}{1.75} - a^2)] \tag{97}$$

2. Perturbation in K_r

The calculation of the formulas for the parameters K_r, K_y, a and b is similar to the calculation for K_ψ. Therefore in the following sections only the main results are presented. The system equations for a change in K_r are

$$\begin{aligned} \dot{\psi} &= r \\ \dot{r} &= ar + a_3 r^3 + b\delta \\ \dot{y} &= \sin\psi \end{aligned} \tag{98}$$

$$\delta = \delta_{sat} \tanh\left(\frac{\delta_0}{\delta_{sat}}\right) \tag{99}$$

$$\delta_0 = K_\psi \psi + cK_r r + K_y y$$

The Jacobian matrix is

$$A = \begin{bmatrix} 0 & 1 & 0 \\ -\alpha_1 & [(1-c)a - c\alpha_2] & -\alpha_0 \\ 1 & 0 & 0 \end{bmatrix} \tag{100}$$

The eigenvalues of the Jacobian matrix are calculated at the bifurcation point from equation (38).

$$\begin{aligned} \lambda_{1,2} &= \pm j\sqrt{\alpha_1} \\ \lambda_3 &= -\frac{\alpha_0}{\alpha_1} \end{aligned} \tag{101}$$

The state vector is presented in normal coordinates where z_3 corresponds to λ_3.

$$\begin{aligned} \psi &= z_1 \\ r &= -\sqrt{\alpha_1}\, z_2 \\ y &= \frac{1}{\sqrt{\alpha_1}} z_2 \end{aligned} \tag{102}$$

The system equation in normal coordinates are.

$$\begin{aligned} \dot{z}_1 &= \beta'\epsilon z_1 - (\omega'\epsilon + \sqrt{\alpha_1})\, z_2 + r_{11} z_1^3 + r_{12} z_1^2 z_2 + r_{13} z_1 z_2^2 + r_{14} z_2^3 \\ \dot{z}_2 &= (\omega'\epsilon + \sqrt{\alpha_1})\, z_1 - \beta'\epsilon z_2 + r_{21} z_1^3 + r_{22} z_1^2 z_2 + r_{23} z_1 z_2^2 + r_{24} z_2^3 \end{aligned} \tag{103}$$

where,

$$\beta = -\frac{\alpha_1^3(\alpha_2 + a)}{2(\alpha_1^3 + \alpha_0^2)} = -0.45428(1.75\omega_n + a)$$
$$\omega = -\frac{\alpha_0\alpha_1^{3/2}(\alpha_2 + a)}{2(\alpha_1^3 + \alpha_0^2)} = -0.1441(1.75\omega_n + a) \quad \textbf{(104)}$$

The coefficients of the third order expansion terms are.

$$r_{11} = \frac{\alpha_0\alpha_1^2}{\alpha_0^2 + \alpha_1^3}\left[\frac{1}{3b^2\delta_{sat}^2}\alpha_1^2 - \frac{1}{6}\right] \quad \textbf{(105)}$$

$$r_{12} = -\frac{a}{b^2\delta_{sat}^2}\frac{\alpha_0\alpha_1^{7/2}}{\alpha_0^2 + \alpha_1^3} \quad \textbf{(106)}$$

$$r_{13} = \frac{a^2}{b^2\delta_{sat}^2}\frac{\alpha_0\alpha_1^3}{\alpha_0^2 + \alpha_1^3} \quad \textbf{(107)}$$

$$r_{14} = -\frac{\alpha_0\alpha_1^{5/2}}{\alpha_0^2 + \alpha_1^3}\left[\frac{a^3}{3b^2\delta_{sat}^2} + a_3\right] \quad \textbf{(108)}$$

$$r_{21} = -\frac{1}{\alpha_0^2 + \alpha_1^3}\left[\frac{\alpha_1^{11/2}}{3b^2\delta_{sat}^2} + \frac{\alpha_0^2\alpha_1^{1/2}}{6}\right] \quad \textbf{(109)}$$

$$r_{22} = -\frac{a}{b^2\delta_{sat}^2}\frac{\alpha_1^4}{\alpha_0^2 + \alpha_1^3} \quad \textbf{(110)}$$

$$r_{23} = -\frac{a^2}{b^2\delta_{sat}^2}\frac{\alpha_1^{9/2}}{\alpha_0^2+\alpha_1^3} \tag{111}$$

$$r_{24} = \frac{\alpha_1^4}{\alpha_0^2+\alpha_1^3}\left[a_3+\frac{a^3}{3b^2\delta_{sat}^2}\right] \tag{112}$$

The cubic coefficients **K** and **M** are obtained after averaging ,

$$K=0.052824[13.8675a_3\omega_n^3-0.5\,\omega_n+\frac{2.15}{b^2d_{sat}^2}(\omega_n^3+2.15a\omega_n^2)(2.15\,\omega_n^2+a^2)] \tag{113}$$

$$\begin{aligned} M &= 0.01142[20.3337a_3\omega_n^2-0.7331\,\omega_n \\ &\quad +\frac{20.9727\omega_n^4}{b^2\delta_{sat}^2}(a-4.6225\,\omega_n)(2.15\,\omega_n^2+a^2)] \end{aligned} \tag{114}$$

3. Perturbation in K_v

The formulas for perturbations in K_v are presented in this section. The equations of motion are.

$$\begin{aligned} \dot{\psi} &= r \\ \dot{r} &= ar+a_3r^3+b\delta \\ \dot{y} &= \sin\psi \end{aligned} \tag{115}$$

$$\delta = \delta_{sat}\tanh\left(\frac{\delta_0}{\delta_{sat}}\right) \tag{116}$$

$$\delta_0 = K_\psi\psi+K_r r+cK_y y$$

The Jacobian matrix.

$$A = \begin{bmatrix} 0 & 1 & 0 \\ -\alpha_1 & -\alpha_2 & -c\alpha_0 \\ 1 & 0 & 0 \end{bmatrix} \tag{117}$$

The eigenvalues at the bifurcation point ,

$$\begin{aligned} \lambda_{1,2} &= \mp j\sqrt{\alpha_1} \\ \lambda_2 &= \alpha_2 \end{aligned} \tag{118}$$

The state equations in normal coordinates,

$$\begin{aligned} \psi &= z_1 \\ r &= -\sqrt{\alpha_1}\, z_2 \\ y &= \frac{1}{\sqrt{\alpha_1}} z_2 \end{aligned} \tag{119}$$

The normalized equations of motion,

$$\begin{aligned} \dot{z}_1 &= \beta'\epsilon z_1 - \left(\omega'\epsilon + \sqrt{\alpha_1}\right) z_2 + r_{11}z_1^3 + r_{12}z_1^2 z_2 + r_{13}z_1 z_2^2 + r_{14}z_2^3 \\ \dot{z}_2 &= \left(\omega'\epsilon + \sqrt{\alpha_1}\right) z_1 + \beta'\epsilon z_2 + r_{21}z_1^3 + r_{22}z_1^2 z_2 + r_{23}z_1 z_2^2 + r_{24}z_2^3 \end{aligned} \tag{120}$$

where β' and ω' are given by,

$$\begin{aligned} \beta' &= \frac{\alpha_0}{2(\alpha_1 + \alpha_2^2)} = 0.0959\,\omega_n \\ \omega' &= \frac{\alpha_0\alpha_2}{2\sqrt{\alpha_1}(\alpha_1 + \alpha_2^2)} = 0.1145\,\omega_n \end{aligned} \tag{121}$$

The coefficients for the third order terms,

$$r_{11} = -\frac{\alpha_1 \alpha_2}{\alpha_1^2 + \alpha_2^2}\left(\frac{1}{6} - \frac{\alpha_1^2}{3b^2\delta_{sat}^2}\right) \tag{122}$$

$$r_{12} = -\frac{a}{b^2\delta_{sat}^2}\frac{\alpha_1^{5/2}\alpha_2}{\alpha_1 + \alpha_2^2} \tag{123}$$

$$r_{13} = \frac{a^2}{b^2\delta_{sat}^2}\frac{\alpha_1^2\alpha_2}{\alpha_1 + \alpha_2^2} \tag{124}$$

$$r_{14} = -\frac{\alpha_1^{3/2}\alpha_2}{\alpha_1 + \alpha_2^2}\left(a_3 + \frac{a^3}{3b^2\delta_{sat}^2}\right) \tag{125}$$

$$r_{21} = -\frac{\alpha_2\sqrt{\alpha_1}}{\alpha_2^2 + \alpha_1}\left(\frac{1}{3b^2\delta_{sat}^2}\frac{\alpha_1^3}{\alpha_2} + \frac{\alpha_2}{6}\right) \tag{126}$$

$$r_{22} = \frac{a}{b^2\delta_{sat}}\frac{\alpha_1^3}{\alpha_1 + \alpha_2^2} \tag{127}$$

$$r_{23} = -\frac{a^2}{b^2\delta_{sat}^2}\frac{\alpha_1^{5/2}}{\alpha_1 + \alpha_2^2} \tag{128}$$

$$r_{24} = \frac{\alpha_1^2}{\alpha_1 + \alpha_2^2}\left(\frac{a^3}{3b^2\delta_{sat}^2} + a_3\right) \tag{129}$$

The cubic coefficients **K** and **M** ,

$$K = 0.05155\left[6.45 a_3 \omega_n^2 - 0.875\,\omega_n + \frac{2.15\,\omega_n^2}{b^2 \delta_{sat}^2}(1.75\,\omega_n + a)(2.15\,\omega_n^2 + a^2)\right] \quad (130)$$

$$M = 0.3969 a_3 \omega_n^2 + \frac{0.075}{b^2 \delta_{sat}^2}\,\omega_n (1.75 a\,\omega_n - 2.15\,\omega_n)(2.15\,\omega_n^2 + a^2) \quad (131)$$

4. Perturbation in a

The equations of motion.

$$\begin{aligned} \dot{\psi} &= r \\ \dot{r} &= car + a_3 r^3 + b\delta \\ \dot{y} &= \sin\psi \end{aligned} \quad (132)$$

where.

$$\delta = \delta_{sat} \tanh\left(\frac{\delta_0}{\delta_{sat}}\right) \quad (133)$$

$$\delta_0 = K_\psi \psi + K_r r - K_y y$$

The Jacobian matrix.

$$A = \begin{bmatrix} 0 & 1 & 0 \\ \alpha_1 & a(c \quad 1) & \alpha_2 & \alpha_0 \\ 1 & 0 & 0 \end{bmatrix} \quad (134)$$

The eigenvalues at the bifurcation point.

$$\begin{aligned} \lambda_{1,2} &= \pm j\sqrt{\alpha_1} \\ \lambda_3 &= \alpha_0 \\ &= \alpha_1 \end{aligned} \quad (135)$$

and the state equations in normalized coordinates.

$$\psi = z_1$$

$$r = -\sqrt{\alpha_1}\, z_2 \qquad (136)$$

$$y = \frac{1}{\sqrt{\alpha_1}} z_2$$

The normalized equations of motion in the neighborhood of the bifurcation point.

$$\begin{aligned} \dot{z}_1 &= \beta' \epsilon z_1 - \left(\omega' \epsilon + \sqrt{\alpha_1}\right) z_2 + r_{11} z_1^3 + r_{12} z_1^2 z_2 + r_{13} z_1 z_2^2 + r_{14} z_2^3 \\ \dot{z}_2 &= \left(\omega' \epsilon + \sqrt{\alpha_1}\right) z_1 - \beta \epsilon z_2 + r_{21} z_1^3 + r_{22} z_1^2 z_2 + r_{23} z_1 z_2^2 + r_{24} z_2^3 \end{aligned} \qquad (137)$$

$$\begin{aligned} \beta' &= -\frac{a}{2} \frac{\alpha_1^3}{\alpha_1^3 + \alpha_0^2} = -0.454a \\ \omega' &= -\frac{a}{2} \frac{\alpha_0 \alpha_1^{3/2}}{\alpha_1^3 + \alpha_0^2} = -0.1441a \end{aligned} \qquad (138)$$

The coefficients of nonlinear terms.

$$r_{11} = \frac{\alpha_0 \alpha_1^{3/2}}{\alpha_0^2 + \alpha_1^3} \left(\frac{1}{3b^2 \delta_{sat}^2} \alpha_1^{5/2} - \frac{\sqrt{\alpha_1}}{6} \right) \qquad (139)$$

$$r_{12} = \frac{1}{b^2 \delta_{sat}^2} \frac{\alpha_0 \alpha_1^{7/2}}{\alpha_0^2 + \alpha_1^3} \left(\sqrt{\alpha_1}(\alpha_2 + a) - \frac{\alpha_0}{\sqrt{\alpha_1}} \right) \qquad (140)$$

$$r_{13} = \frac{1}{b^2 \delta_{sat}^2} \frac{\alpha_0 \alpha_1}{\alpha_0^2 + \alpha_1^3} \left((\alpha_2 + a)^2 \alpha_1^2 - \alpha_0^2 + 2\alpha_1 \alpha_0 (\alpha_2 + a) \right) \qquad (141)$$

$$r_{14} = \frac{\alpha_0 \alpha_1^{3/2}}{\alpha_0^2 + \alpha_1^3}\{-a_3\alpha_1 - \frac{1}{3b^2\delta_{sat}^2\sqrt{\alpha_1}}((\alpha_2+a)^2\alpha_1^{3/2} - 3(\alpha_2+a)^2\alpha_1^{1/2}\alpha_0 + 3\alpha_0^2\alpha_1^{-1/2}(\alpha_2+a) - \frac{\alpha_0^3}{\alpha_1^{3/2}}\} \quad (142)$$

$$r_{21} = \frac{\alpha_0 \alpha_1^{3/2}}{\alpha_0^2 + \alpha_1^3}\left(-\frac{1}{3b^2\delta_{sat}^2}\frac{\alpha_1^4}{\alpha_0} - \frac{\alpha_0}{6\alpha_1}\right) \quad (143)$$

$$r_{22} = \frac{1}{b^2\delta_{sat}^2}\frac{\alpha_1^5}{\alpha_0^2 + \alpha_1^3}\left((\alpha_2+a) - \frac{\alpha_0}{\alpha_1}\right) \quad (144)$$

$$r_{23} = \frac{1}{b^2\delta_{sat}^2}\frac{\alpha_1^{5/2}}{\alpha_0^2 + \alpha_1^3}(-(\alpha_2+a)^2\alpha_1^2 - \alpha_0^2 + 2\alpha_1\alpha_0(\alpha_2+a)) \quad (145)$$

$$r_{24} = \frac{\alpha_0 \alpha_1^{3/2}}{\alpha_0^2 + \alpha_1^3}[a_3\frac{\alpha_1^{5/2}}{\alpha_0} + \frac{1}{3b^2\delta_{sat}^2}\frac{\alpha_1}{\alpha_0} \{(\alpha_2+a)^3\alpha_1^{3/2} - 3(\alpha_2+a)^2\alpha_1^{1/2}\alpha_0 + 3\alpha_0^2\alpha_1^{-1/2}(\alpha_2+a) - \frac{\alpha_0^3}{\alpha_1^{3/2}}\}] \quad (146)$$

The cubic coefficients **K** and **M** are

$$K = 0.03603[-0.7331\omega_n + 6.7779a_3\omega_n^2 + \frac{1}{b^2\delta_{sat}^2}(6.7779\omega_n^5 + (\frac{1}{1.4662\omega_n} + 14.5725\omega_n^4)(-\omega_n^6 + (4.3\omega_n^5 - 1)(1.75\omega_n + a)) + \frac{0.7166}{\omega_n}(1.884\omega_n^2 + 1.4663a\omega_n)^3)] \quad (147)$$

$$M = 0.03603\left[-\frac{\omega_n}{4.3} + 6.45 a_3 \omega_n^2 3 \right.$$
$$+ \frac{1}{b^2 \delta_{sat}^2} [-21.3675\omega_n^5 + 2.15\omega_n^2(-7.6314\omega_n^6 - 11.8787 a \omega_n + 2.15^2 a^2 \omega_n^4) \quad (148)$$
$$-2.15^2 \omega_n^4 (1.884 \omega_n^2 + 2.15^{1/2} a \omega_n)$$
$$\left. + \frac{1}{4.3988 \omega_n} (1.884 \omega_n^2 + 2.15^{1/2} a \omega_n)^3] \right]$$

5. Perturbation in b

The equations of motion are,

$$\begin{aligned} \psi &= r \\ \dot{r} &= ar + a_3 r^3 + cb\delta \\ \dot{y} &= \sin\psi \end{aligned} \quad (149)$$

where,

$$\delta = \delta_{sat} \tanh\left(\frac{\delta_0}{\delta_{sat}} \right) \quad (150)$$
$$\delta_0 = K_\psi \psi + K_r r + K_y y$$

and the Jacobian is,

$$A = \begin{bmatrix} 0 & 1 & 0 \\ -c\alpha_1 & (1-c)a - c\alpha_2 & -c\alpha_0 \\ 1 & 0 & 0 \end{bmatrix} \quad (151)$$

The eigenvalues are,

$$\lambda_{1,2} = \mp j\sqrt{\frac{\alpha_0 + a\alpha_1}{\alpha_2 + a}}$$
$$\lambda_3 = \frac{\alpha_0}{\alpha_1} \tag{152}$$

The normal coordinate transformation is,

$$\psi = z_1$$
$$r = -\sqrt{\frac{\alpha_o + a\alpha_1}{\alpha_2 + a}}\, z_2 \tag{153}$$
$$y = \sqrt{\frac{\alpha_2 + a}{\alpha_0 + a\alpha_1}}\, z_2$$

The normalized equations of motion are,

$$\dot{z}_1 = \beta'\epsilon z_1 - \left(\omega'\epsilon + \sqrt{\frac{\alpha_0 + a\alpha_1}{\alpha_2 + a}}\right) z_2 + r_{11}z_1^3 + r_{12}z_1^2 z_2 + r_{13}z_1 z_2^2 + r_{14}z_2^3$$
$$\dot{z}_2 = \left(\omega'\epsilon + \sqrt{\frac{\alpha_0 + a\alpha_1}{\alpha_2 + a}}\right) z_1 + \beta'\epsilon z_2 + r_{21}z_1^3 + r_{22}z_1^2 z_2 + r_{23}z_1 z_2^2 + r_{24}z_2^3 \tag{154}$$

where β' and ω' are,

$$\beta' = -\frac{\alpha_1^2(\alpha_0 + \alpha_1 a)(\alpha_2 + a)}{2(\alpha_0 + \alpha_1 a)\alpha_1^2 + \alpha_0^2(\alpha_2 + a)} = -\frac{2.15^2(\omega_n + 2.15a)(1.75\omega_n + a)}{10.995\omega_n + 20.8767a} \tag{155}$$

$$\omega' = \frac{\alpha_1}{2}\sqrt{\frac{\alpha_2 + a}{\alpha_0 + a\alpha_1}}\left(1 - \frac{\alpha_0(\alpha_0 + a\alpha_1)(\alpha_2 + a)}{(\alpha_0 + a\alpha_1)\alpha_1^2 + \alpha_0^2(\alpha_2 + a)}\right) \tag{156}$$

$$= 1.075\sqrt{\frac{1.75\omega_n + a}{\omega_n + 2.15a}}\left(1 - \frac{(\omega_n + 2.15a)(1.75\omega_n + a)}{\omega_n(6.3725\omega_n + 10.9384a)}\right)$$

The coefficients of third order terms are given in terms of the dummy coefficient Ω ,

$$\Omega = \frac{\alpha_1\alpha_0(\alpha_2 + a)^{1/2}(\alpha_0 + a\alpha_1)^{1/2}}{\alpha_0^2(\alpha_2 + a) + \alpha_1^2(\alpha_0 + a\alpha_1)} \tag{157}$$

$$r_{11} = \Omega\left(-\frac{1}{6}\sqrt{\frac{\alpha_0 + a\alpha_1}{\alpha_2 + a}} + \frac{\alpha_1^3}{3b^2\delta_{sat}^2}\sqrt{\frac{\alpha_0 + a\alpha_1}{\alpha_2 + a}}\right) \tag{158}$$

$$r_{12} = \Omega\frac{a}{b^2\delta_{sat}^2}\alpha_1^3 \tag{159}$$

$$r_{13} = \Omega\frac{a^2\alpha_1^3}{b^2\delta_{sat}^2}\sqrt{\frac{\alpha_2 + a}{\alpha_0 + a\alpha_1}} \tag{160}$$

$$r_{14} = \Omega\left(-a_3\left(\frac{\alpha_0 + a\alpha_1}{\alpha_2 + a}\right) + \frac{(a\alpha_1)^3}{3b^2\delta_{sat}^2}\left(\frac{\alpha_0 + a\alpha_1}{\alpha_2 + a}\right)^3\right) \tag{161}$$

$$r_{21} = -\Omega\left[\frac{\alpha_0}{6\alpha_1} + \frac{1}{3b^2\delta_{sat}^2}\frac{\alpha_1^4}{\alpha_0}\left(\frac{\alpha_0 + a\alpha_1}{\alpha_2 + a}\right)\right] \tag{162}$$

$$r_{22} = \Omega \frac{c_{crit}}{b^2 \delta_{sat}^2} \frac{a}{\alpha_0} \frac{\alpha_1^4}{\alpha_0} \sqrt{\frac{\alpha_0 + a\alpha_1}{\alpha_2 + a}} \tag{163}$$

$$r_{23} = -\Omega \frac{a^2 \alpha_1^4}{b^2 \delta_{sat}^2} \tag{164}$$

$$r_{24} = \Omega \left(a_3 \frac{\alpha_1}{\alpha_0} \left(\frac{\alpha_0 + a\alpha_1}{\alpha_2 + a} \right)^{3/2} + \frac{a^3}{3b^2 \delta_{sat}^2} \frac{\alpha_1^4}{\alpha_0^2} \sqrt{\frac{\alpha_2 + a}{\alpha_0 + a\alpha_1}} \right) \tag{165}$$

The cubic coefficients **K** and **M** are expressed in terms of the natural frequency ω,

$$K = \frac{\omega_n^2}{8(6.3725\omega_n^2 + a\omega_n + 2.15^2 a)} [2.15a^3 \omega_n \frac{(\omega_n + 2.15a)^2}{1.75\omega_n + a} - 1.075(\omega_n + 2.15a) + \frac{2.15^3 \omega_n^2}{b^2 \delta_{sat}^2} [\![2.15\omega_n^3 (\omega_n + 2.15a)^2 + a(1.75\omega_n + a)(1 + 2.15^2 a^2 \omega_n)]\!]] \tag{166}$$

$$M = \frac{0.2688\sqrt{(1.75\omega_n + a)(\omega_n + 2.15a)}}{(2.9\omega_n + 6.6225a)} [3a_3 \frac{\omega_n + a2.15}{1.75\omega_n + a} - \frac{\omega_n}{4.3} + \frac{1}{b^2 \delta_{sat}^2} [\![2.15^4 \omega_n^3 \frac{\omega_n + 2.15a}{1.75\omega_n + a} - (2.15a^4 \omega_n^5 - 2.15^3 a\omega_n^6 + 2.15^3 a^3 \omega_n^{12} \left(\frac{\omega_n + a2.15}{1.75\omega_n + a} \right)^3]\!]] \tag{167}$$

C. RESULTS

Before we present the results of analytic study of Hopf bifurcation we have to assess the effect of the a_3 term. The a_3 term plays a role in equation (12), and from the nature of the equation we can see that a_3 has to have a negative value. This is because of the softening spring characteristic of the steady state r - δ curve, as shown in Figure 10.

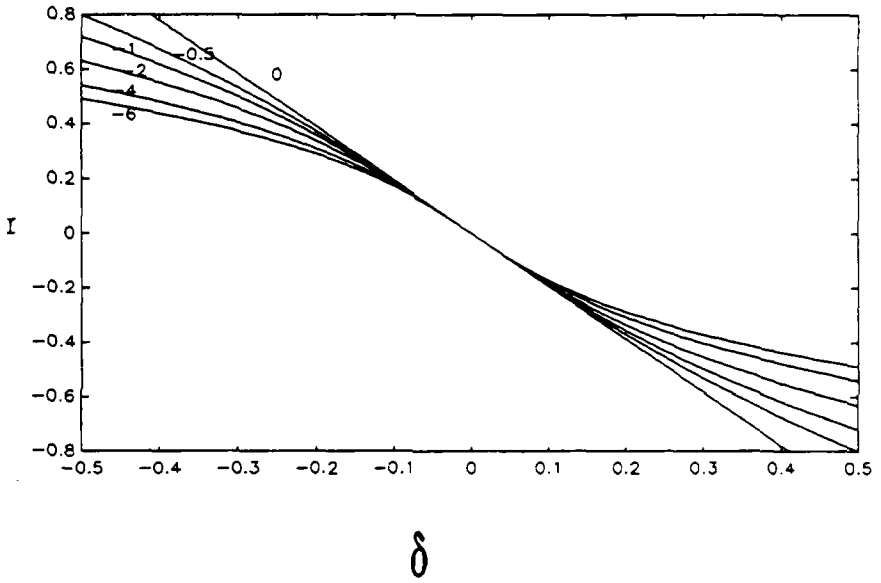

Figure 10 r -δ graph for different a_3 values.

In the previous sections expressions for β' and K were found for equation (89). The value of K depends on only the nonlinear terms and since the eigenvalues of the Jacobian matrix cross the imaginary axis with nonzero speed the term β' is nonzero. Equation (89) has two steady state solutions, one at R=0 which corresponds to the trivial equilibrium solution at zero and one at

$$R_0^2 = -\frac{\beta'}{K}\epsilon \qquad (168)$$

This equilibrium solution corresponds to a periodic solution (limit cycle) in the cartesian coordinates z_1, z_2. From equation (168) we can conclude that.

1. If $\beta' > 0$ then,

a. If $K > 0$, then unstable period solutions coexist with the stable equilibrium for $\epsilon < 0$, and

b. If $K < 0$, then stable period solutions coexist with the unstable equilibrium for $\epsilon > 0$,

2. If $\beta' < 0$ then,

a. If $K > 0$, then unstable period solutions coexist with the stable equilibrium for $\epsilon > 0$, and

b. If $K < 0$, then stable period solutions coexist with the unstable equilibrium for $\epsilon < 0$.

The stable periodic solutions form the supercritical Poincare´ - Andronov - Hopf (PAH) bifurcation, while the unstable periodic solutions form the subcritical PAH bifurcation.The period of the limit cycles is computed by substituting equation (168) in (94)

$$T = \frac{2\pi}{\omega_n + \omega'\epsilon + MR_0^2} = \frac{2\pi}{\omega_n}\left(1 - \frac{\omega' K - \beta' m}{\omega_n K}\epsilon\right) + O(\epsilon^2) \qquad (169)$$

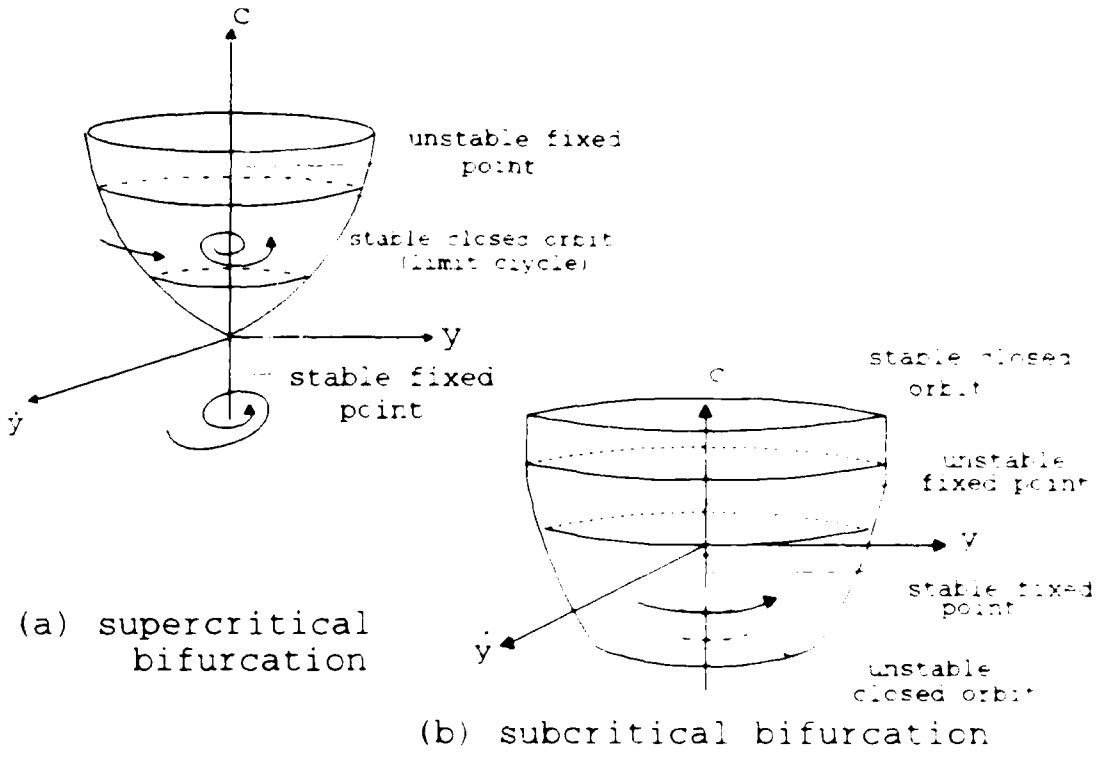

Figure 11 The two general types of Hopf bifurcation.

The existence and stability of periodic solutions in our cases is examined in the following subsections. The graphs of ω' and β' are presented in figures (12) and (13). We note that for **b** and for natural frequency in the range $|a/1.75| < \omega_n < |2.15a|$ the system does not have a complex pair of eigenvalues. Hopf bifurcation does not occur in that interval.

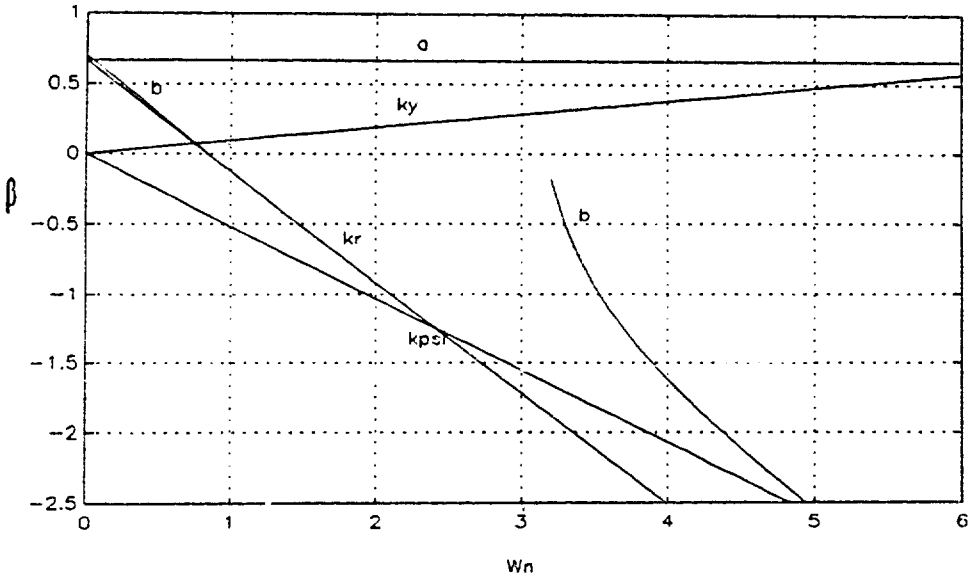

Figure 12 β' versus ω_n.

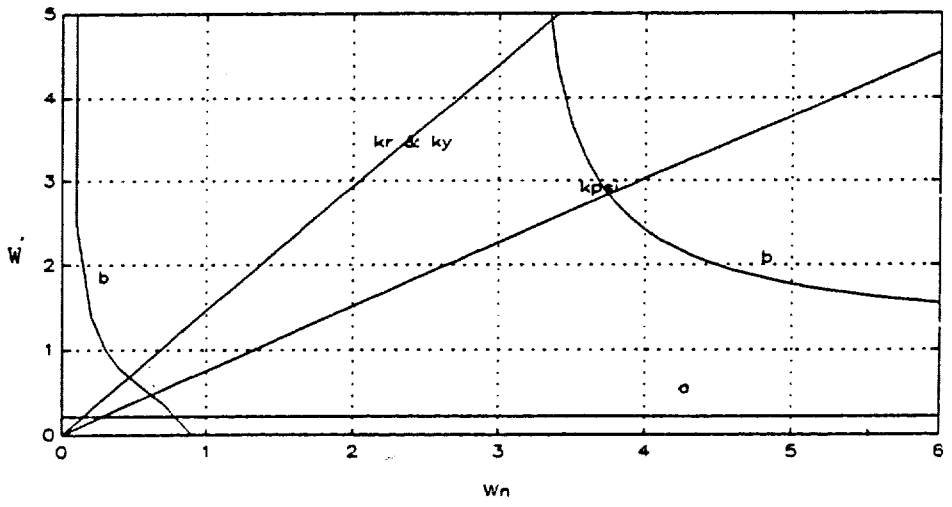

Figure 13 ω' versus ω_n.

1. Perturbation in K_ψ

The graph of β' for K_ψ is shown in figure (13). β' is always negative for K_ψ, and the solutions of equation (91) is presented in figures (14), (15), (16). K is less than zero for low natural frequencies. For those frequencies we get a supercritical Hopf bifurcation and a stable periodic solution exists.However when the natural frequency increases the bifurcation shifts to a subcritical Hopf bifurcation. Figure (14) is obtained for $a_3 = 0$ and various δ_{sat}. Figure (15) is obtained for $a_3 = -3$ and various δ_{sat}. Figure (16) is obtained for $\delta_{sat}=0.4$ and various a_3.When $|a_3|$ increases the domain of the natural frequencies, which causes supercritical Hopf bifurcation, increases as well.

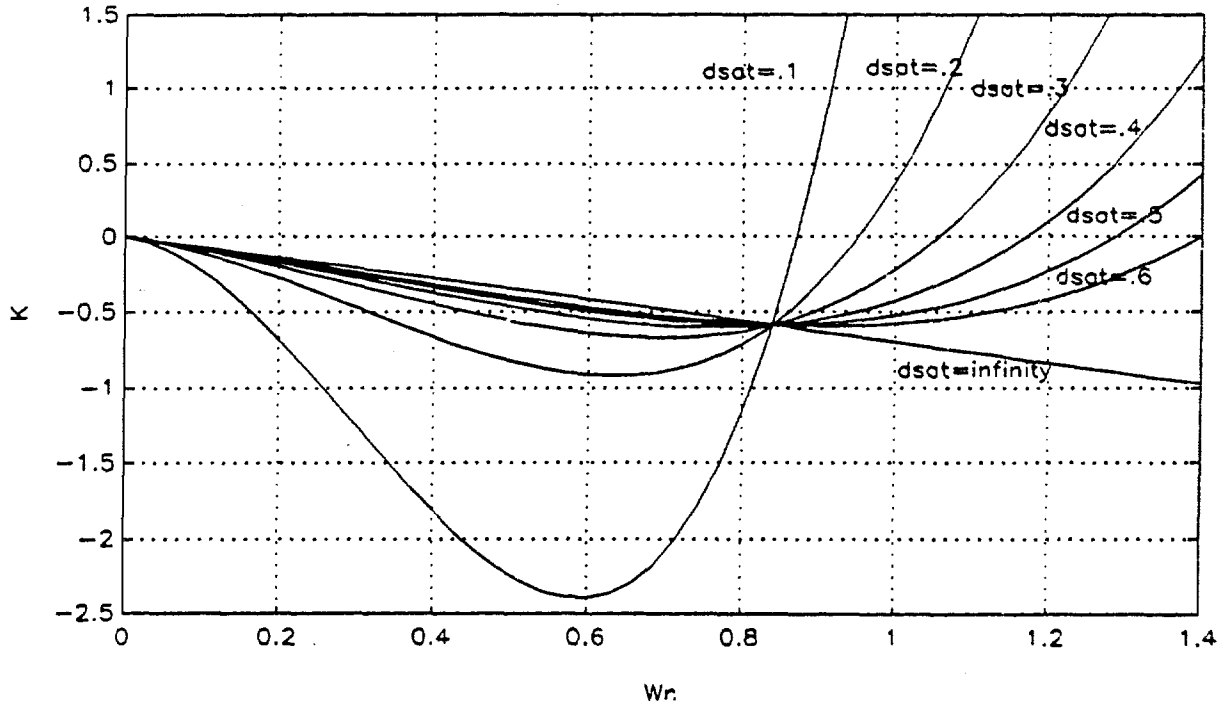

Figure 14 $K_{K\psi}$ versus ω_n for $a_3 = 0$ and various δ_{sat}.

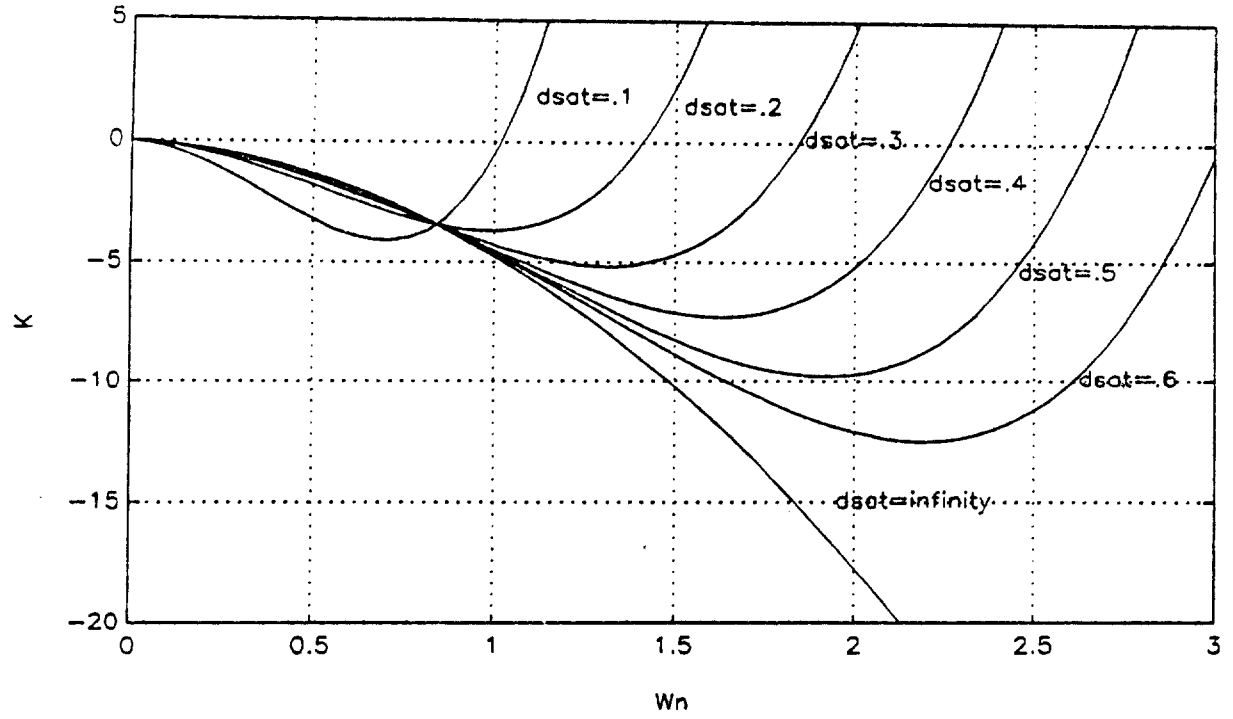

Figure 15 $K_{K\psi}$ versus ω_n for $a_3 = -3$ and various δ_{sat}.

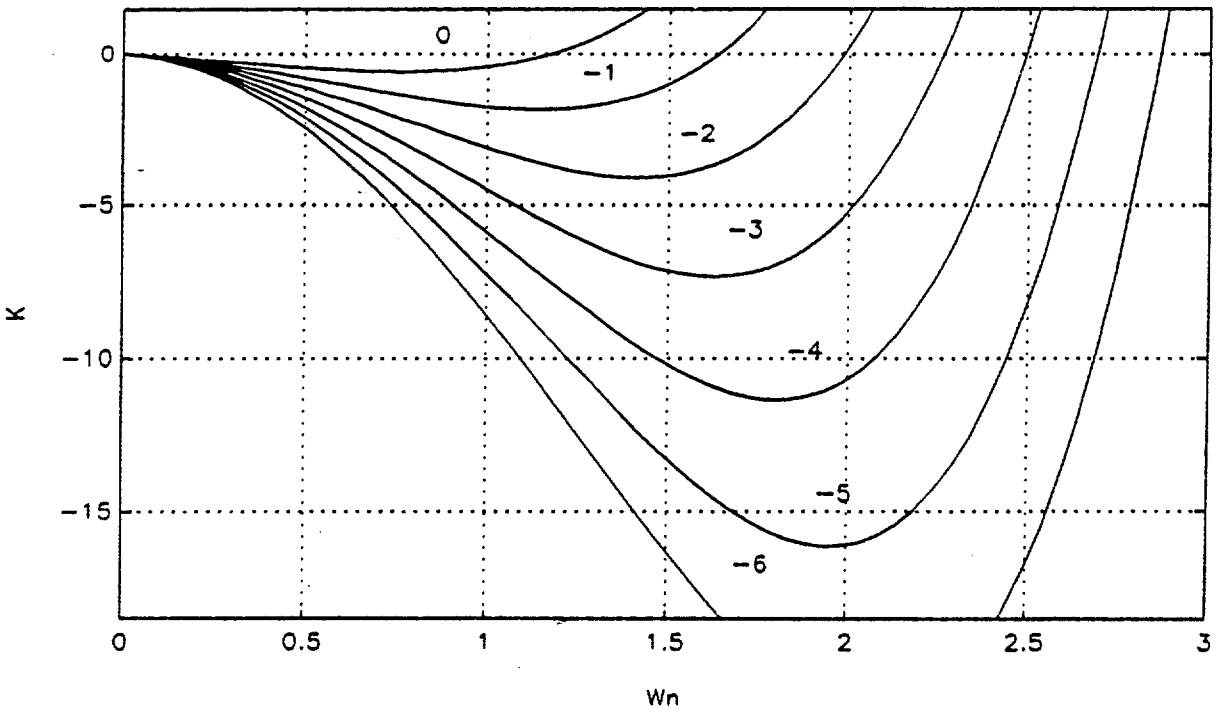

Figure 16 $K_{K\psi}$ versus ω_n for $\delta_{sat}=0.4$ and various a_3.

2. Perturbation in K_r

The term β' for K_r changes its sign at $\omega_n = |a/1.75|$ and can be observed from Figure (12). Therefore, for values of $K<0$ there exists a supercritical Hopf bifurcation whereas subcritical Hopf bifurcation forms when K changes its sign. From Figure (17) it is observed that δ_{sat} does not affect the domain of the natural frequency for supercritical Hopf bifurcation. However, an increase in the $|a_3|$ term increases the domain of supercritical Hopf bifurcation, as can be seen from Figures (18) and (19).

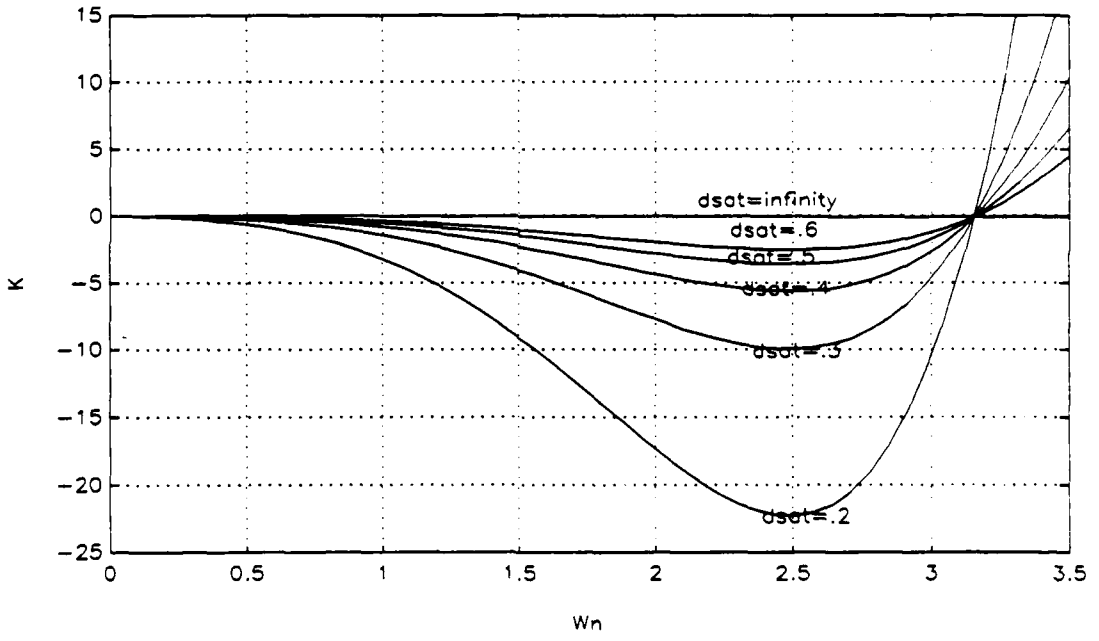

Figure 17 K_{Kr} versus ω_n for $a_3=0$ and various δ_{sat}.

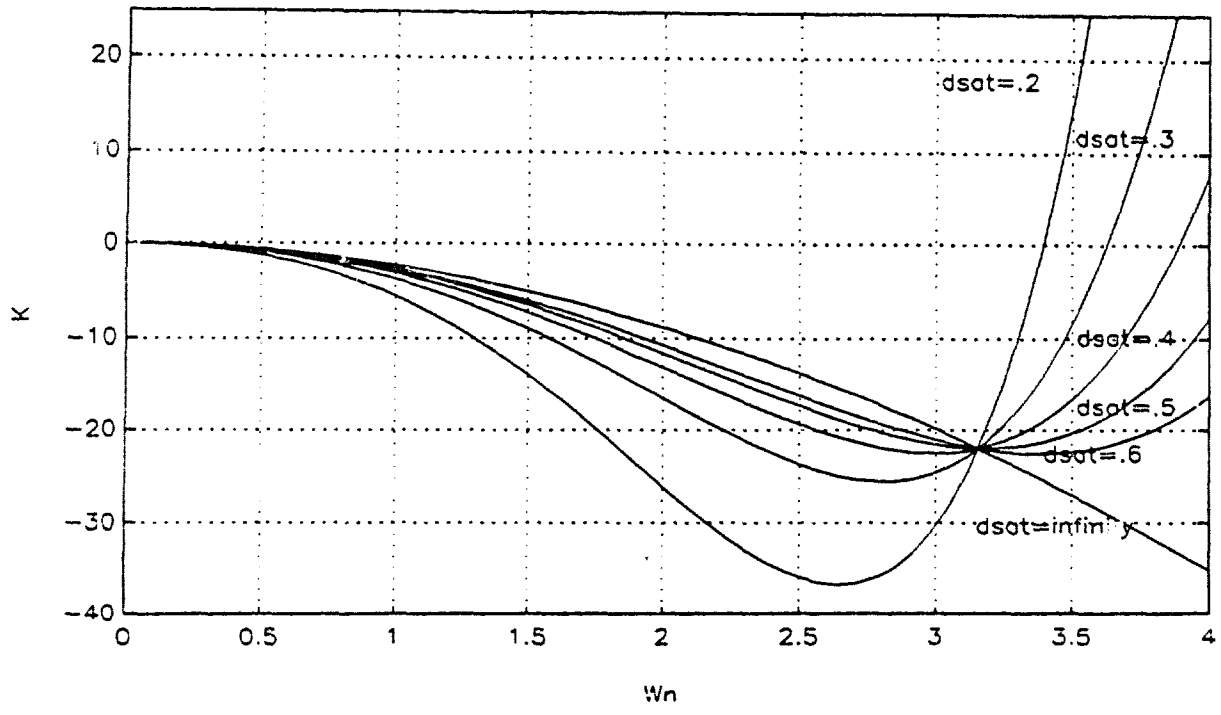

Figure 18 K_{Kr} versus ω_n for a_3=-3 and various δ_{sat}.

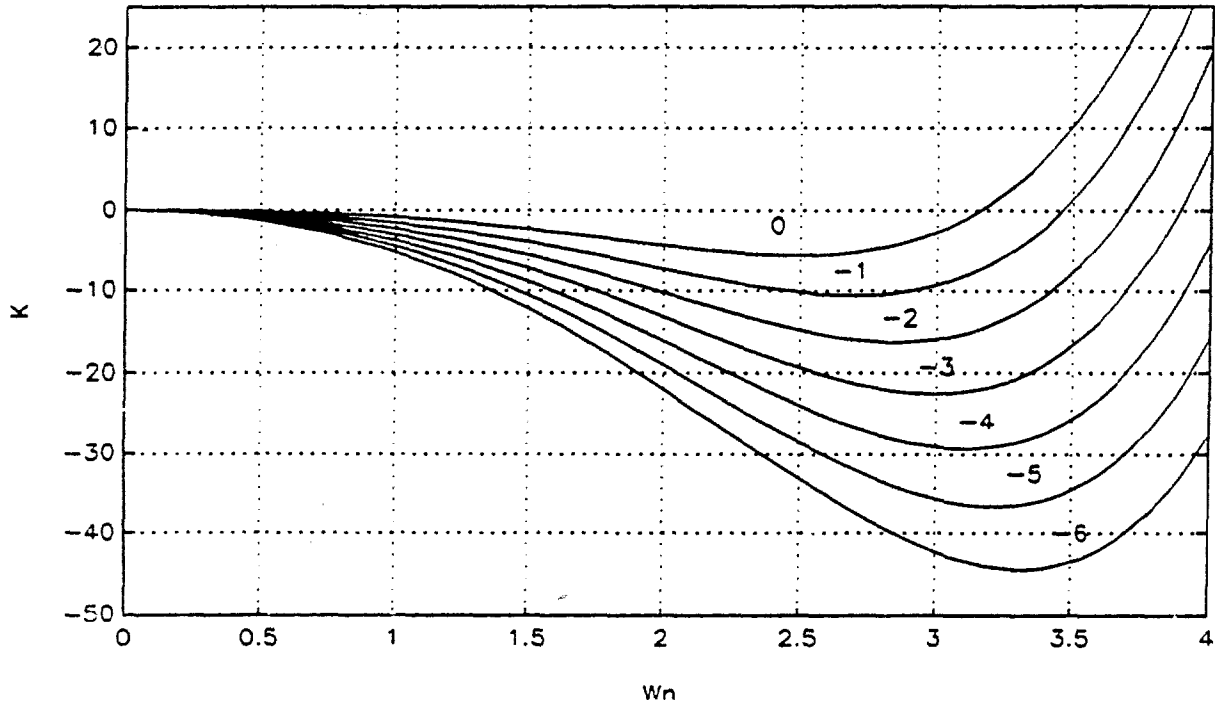

Figure 19 K_{Kr} versus ω_n for δ_{sat}=0.4 and various a_3.

3. Perturbation in K_y

For this case β' is always positive and for $\epsilon > 0$ there exists an unstable equilibrium, therefore for $K < 0$ a supercritical Hopf bifurcation exists. Similarly for $K > 0$ a subcritical Hopf bifurcation exists. An increase in δ_{sat} increases the domain of the supercritical Hopf bifurcation over the natural frequency, see Figure (20). Also an increase in $|a_3|$ increases the domain of the supercritical Hopf bifurcation, see Figures (21), (22).

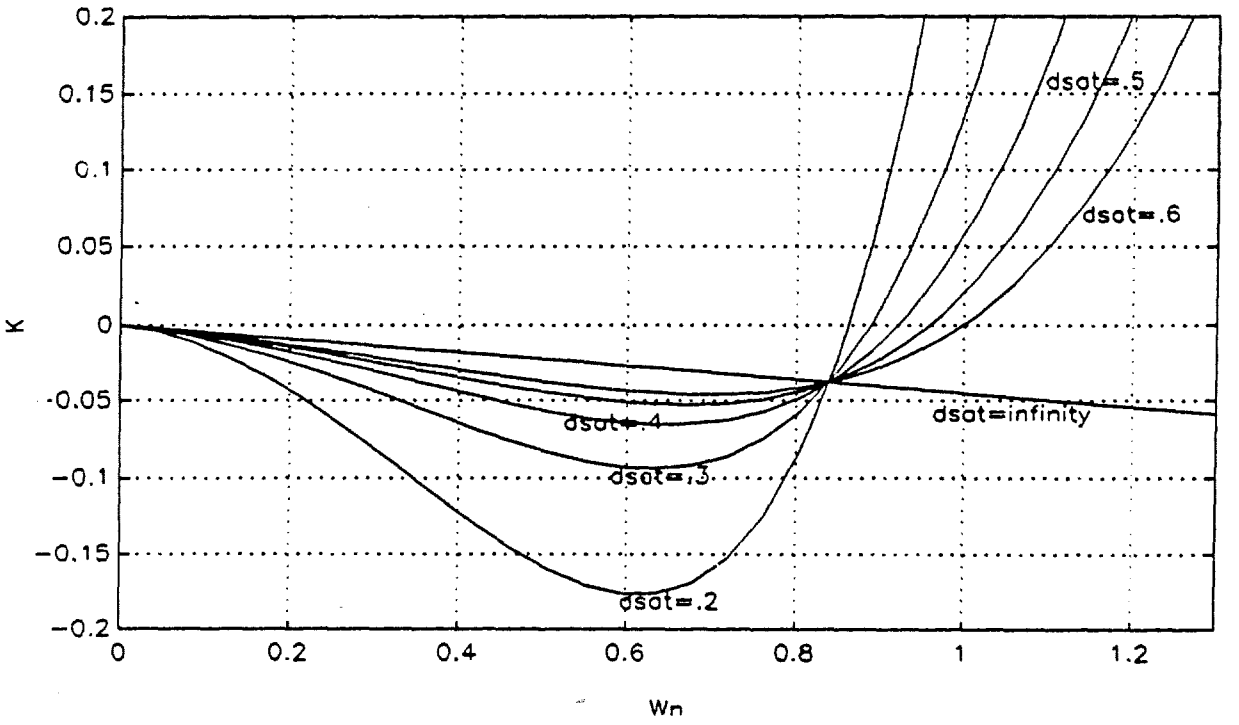

Figure 20 K_{Ky} versus ω_n for $a_3 = 0$ and various δ_{sat}

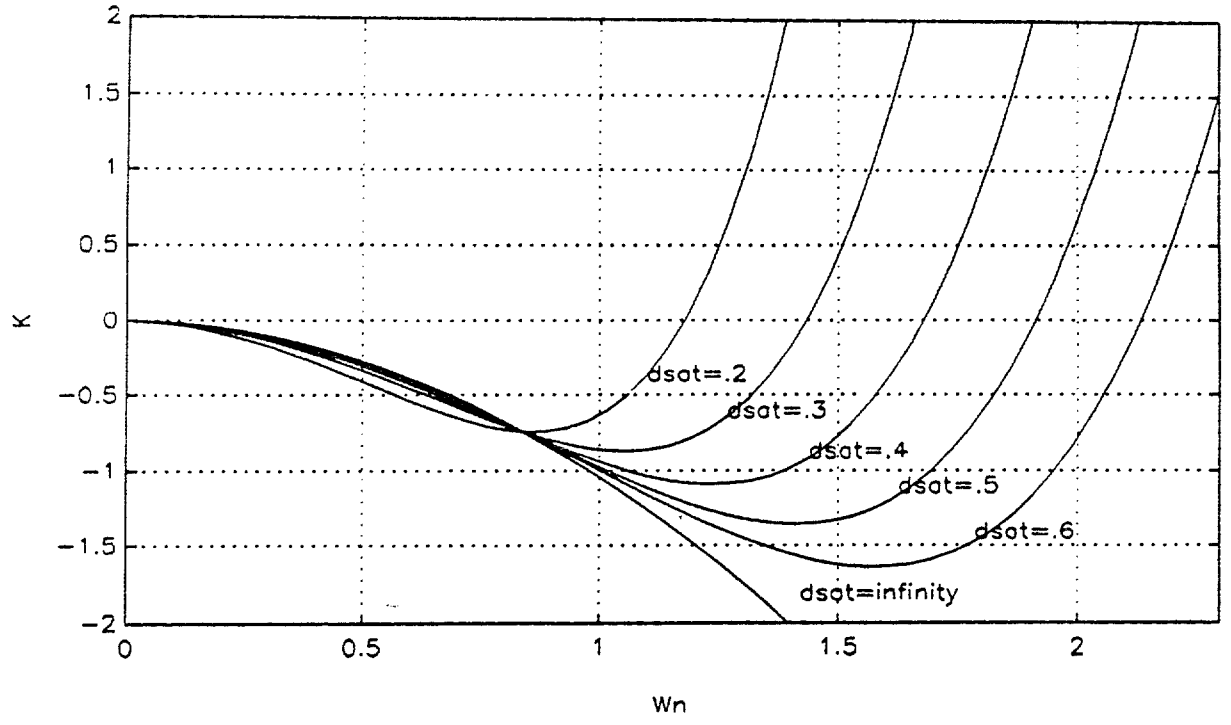

Figure 21 K_{Ky} versus ω_n for $a_3 = -3$ and various δ_{sat}

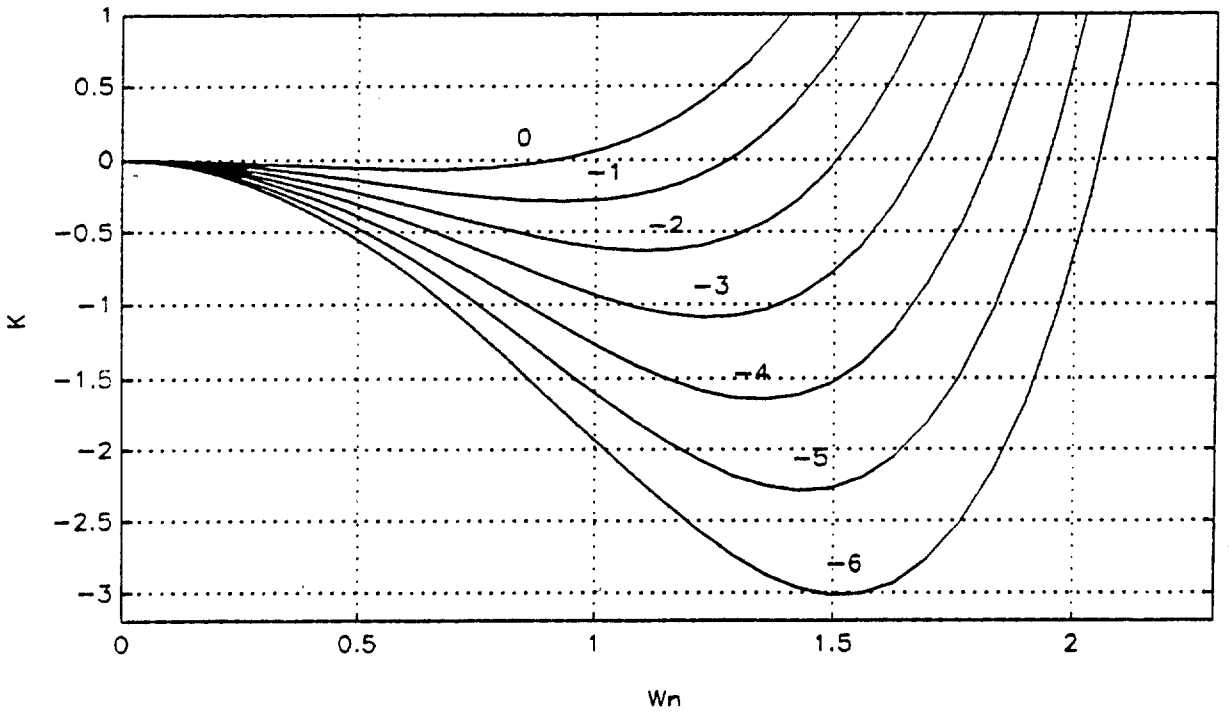

Figure 22 K_{Ky} versus ω_n for $\delta_{sat}=0.4$ and various a_3.

4. Perturbation in a

β' is always positive for this case. For $\epsilon > 0$ and $K < 0$ there exists a stable period solution coexisting with the unstable equilibrium. When $a_3 = 0$, a change in δ_{sat} does not affect the supercritical Hopf bifurcation region of the natural frequency, Figure (23). If a_3 is non zero, an increase in δ_{sat} increases the domain of the natural frequency which causes the supercritical Hopf bifurcation. An increase in $|a_3|$ also increases the domain of the natural frequencies for supercritical Hopf bifurcation, see Figures (24), (25).

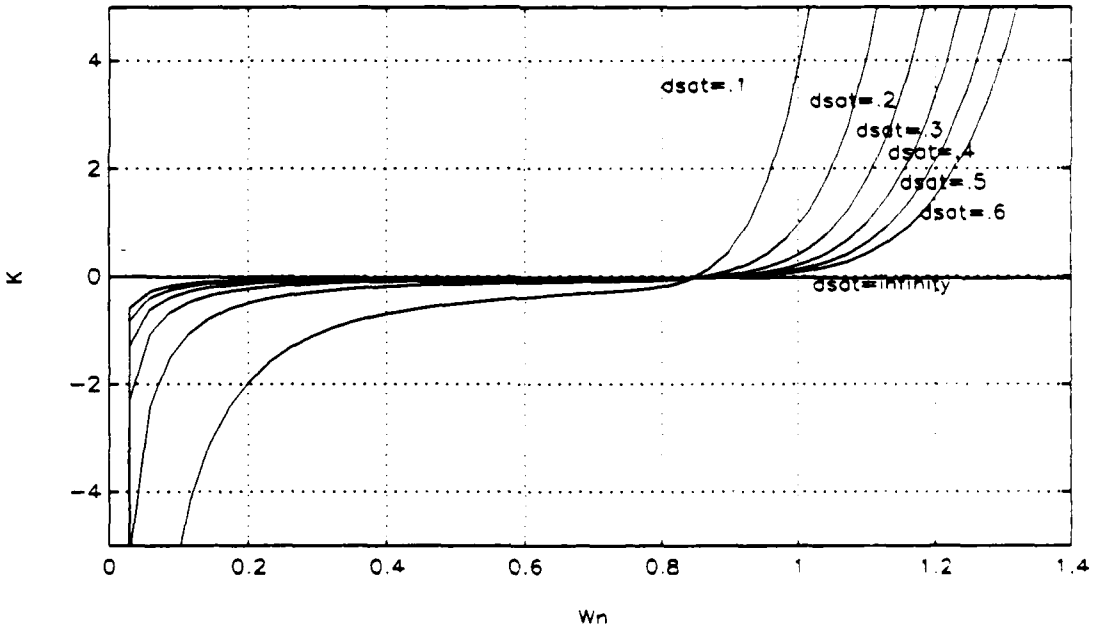

Figure 23 K_a versus ω_n for $a_3 = 0$ and various δ_{sat}

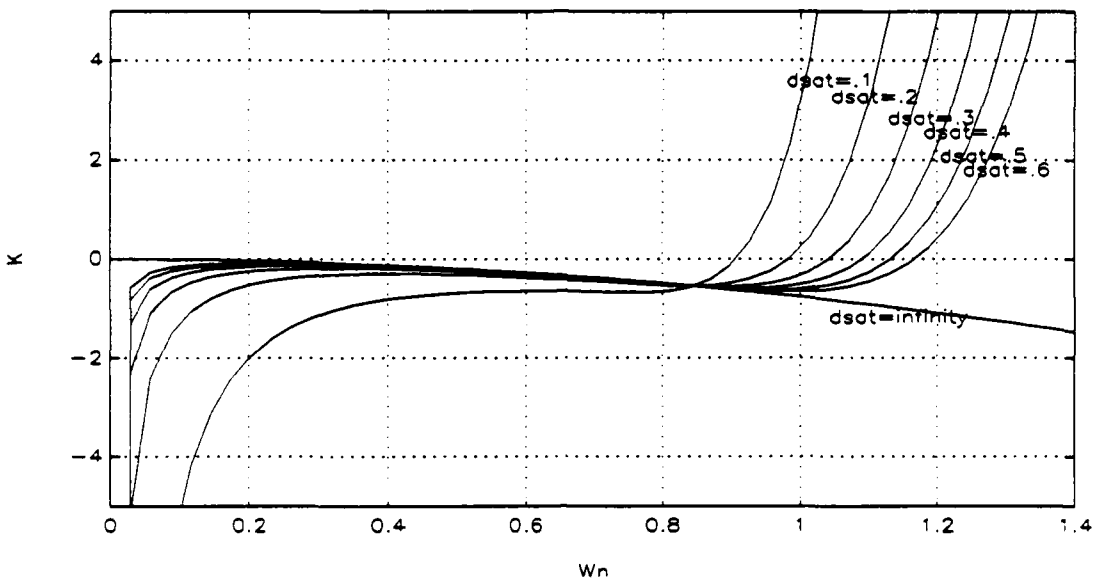

Figure 24 K_a versus ω_n for $a_3 = -3$ and various δ_{sat}

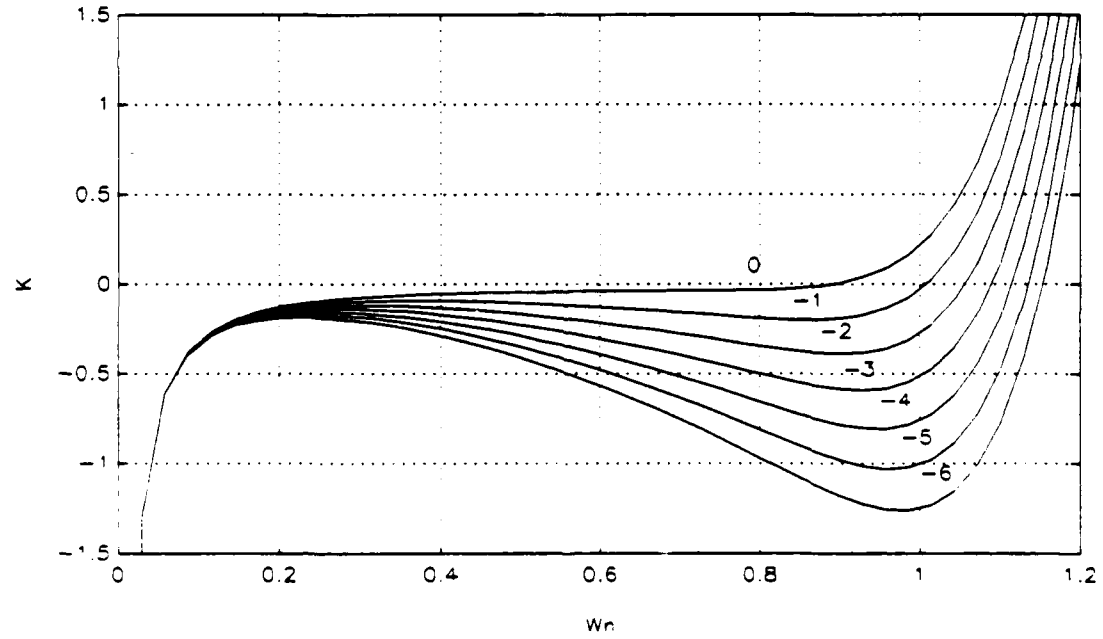

Figure 25 K_a versus ω_n for $\delta_{sat}=0.4$ and various a_3.

5. Perturbation in b

Previously it was shown that there is no Hopf bifurcation in the interval, $|1.75/a| < \omega_n < |2.15a|$ K can be examined in two regions, $0 < \omega_n < |1.75/a|$ and $\omega_n > |21.15a|$. In the first region β' is always negative, $\epsilon > 0$, and K is always negative. In this region only supercritical Hopf bifurcation occurs. Changes in δ_{sat} and $|a_3|$ have no effect in this region, see Figures (26), (27), (28) . For the second region $\beta' < 0$, $\epsilon < 0$, $K < 0$ initially and supercritical Hopf bifurcations exist. For higher natural frequencies, subcritical Hopf bifurcation is observed. Figures (29) and (30) show that changes in δ_{sat} or a_3 have no significant effect.

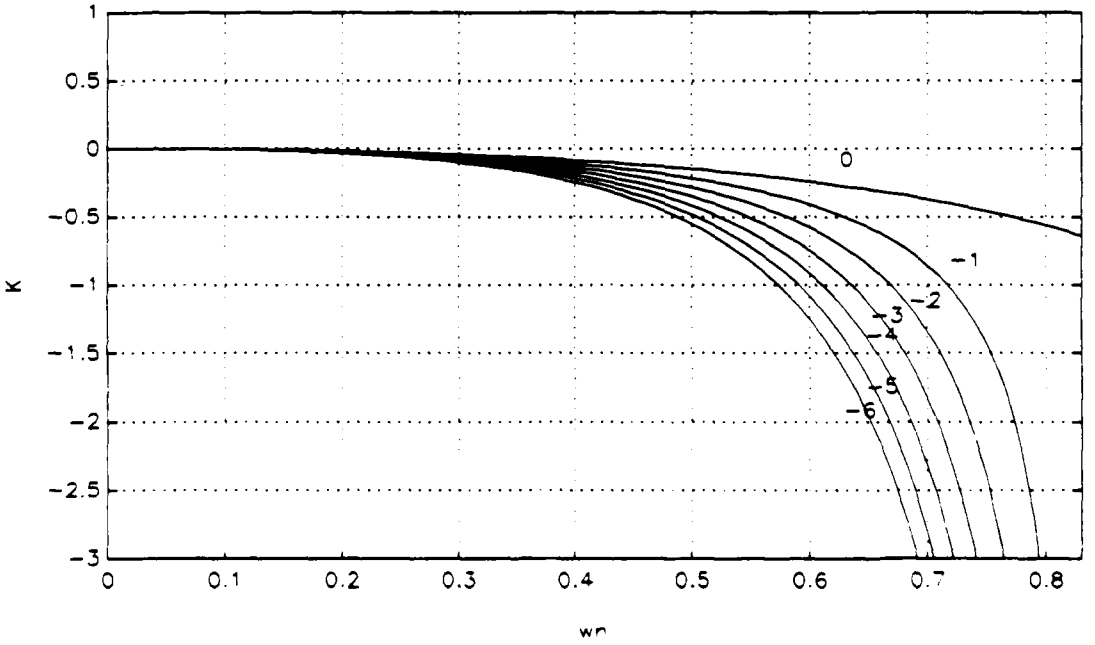

Figure 26 K_b versus ω_n for $\delta_{sat} = 0.4$ and various a_3 for the first region.

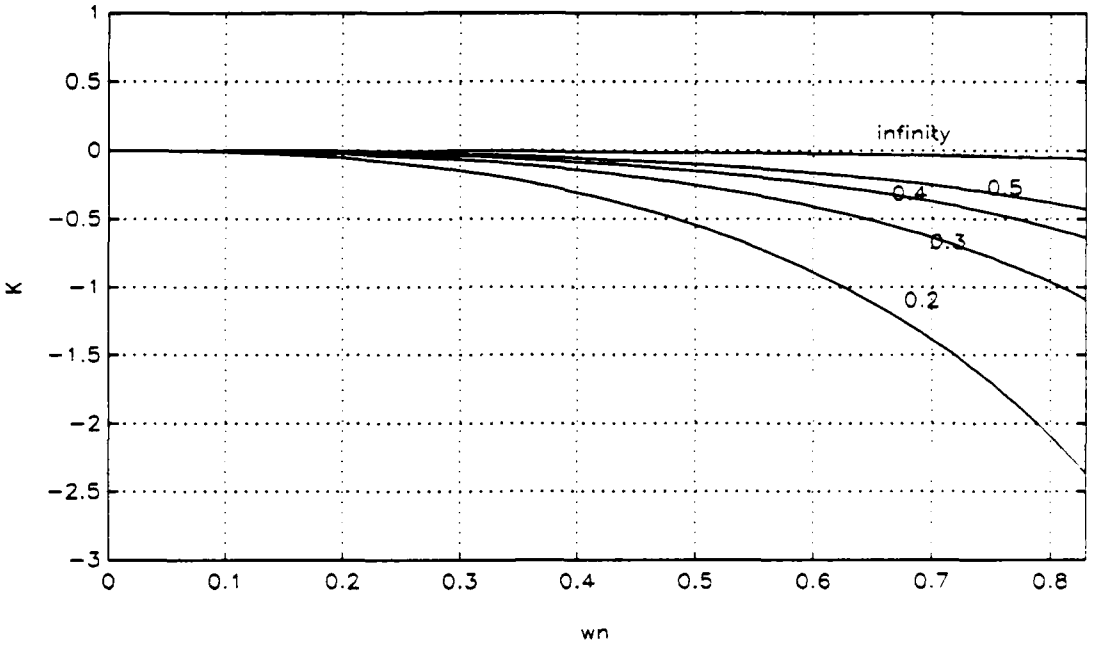

Figure 27 K_b versus ω_n for $a_3 = 0$ and various δ_{sat} for the first region.

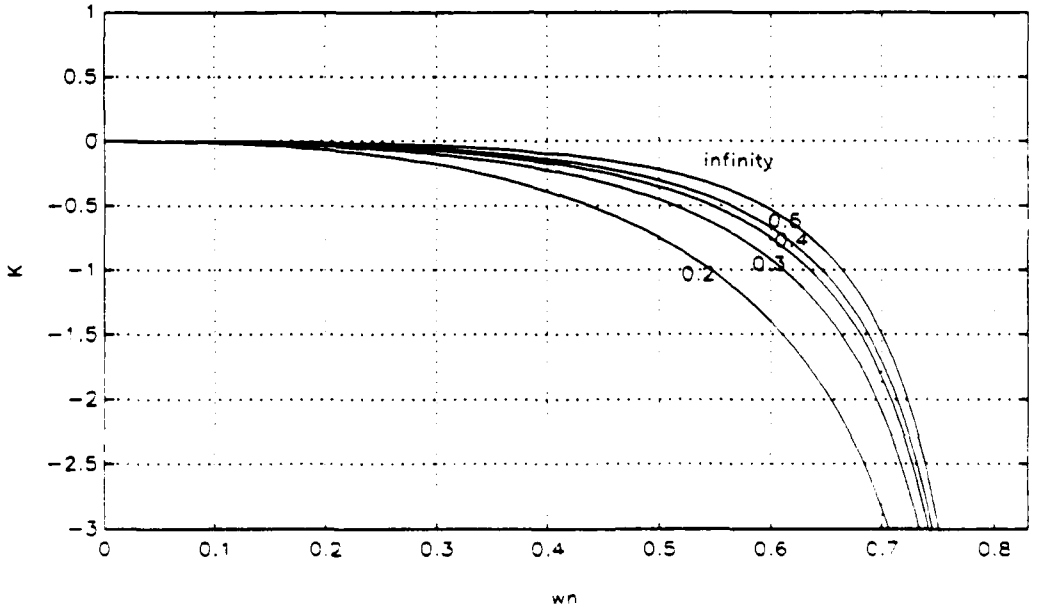

Figure 28 K_b versus ω_n for $a_3 = -3$ and various δ_{sat} for the first region.

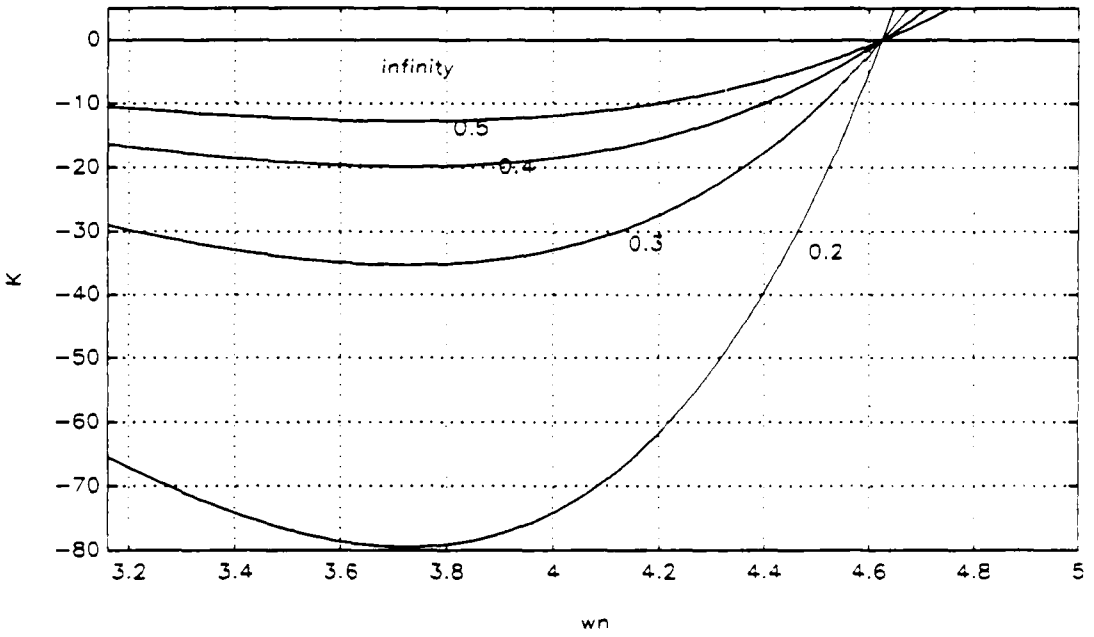

Figure 29 K_b versus ω_n for δ_{sat} =0.4 and various a_3 for the second region.

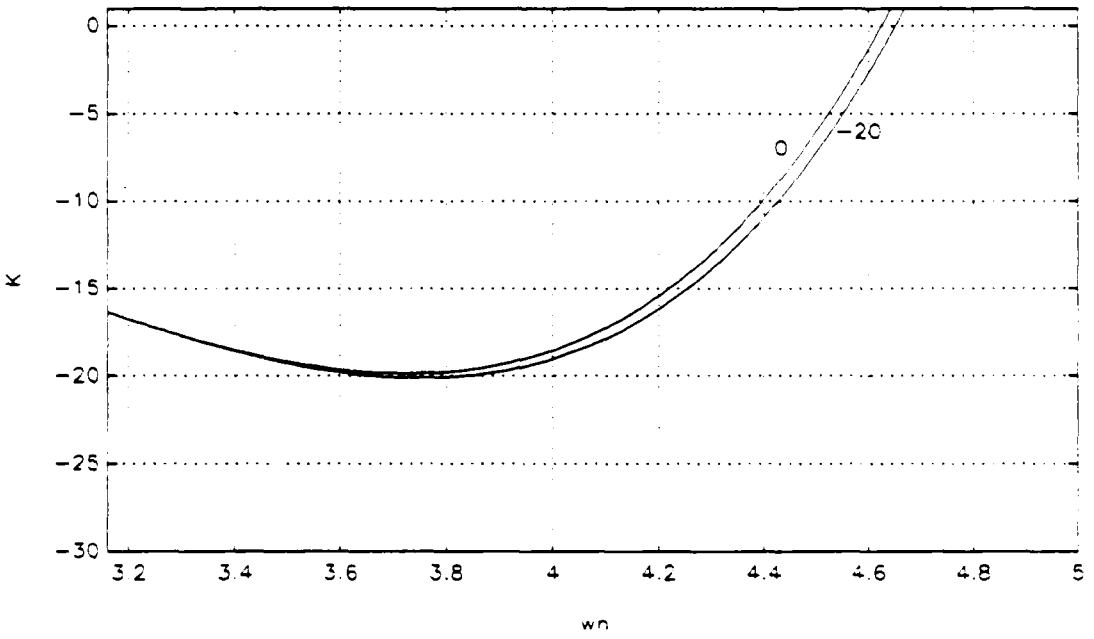

Figure 30 K_b versus ω_n for δ_{sat}= 0.4 and various a_3 for the second region.

IV. SIMULATIONS

To illustrate the dynamics of the Hopf bifurcation we simulated the case in which there is a change in the gain K_y. We compared the simulations with the analytic studies presented in previous chapters. In our case, loss of stability occurs at $c=3.7625$ from stable to unstable while **c** increases its value, as can be observed from Figure (6). In the following simulations we use the typical saturation angle for the rudder of 0.4 radians. The a_3 term is assumed to be zero.

K is less than zero for the natural frequency 0.4 in Figure (20), therefore a supercritical Hopf bifurcation exists in this region. The behavior of this supercritical Hopf bifurcation is simulated in Figures (31), and (32). In Figure (31) $c_{Ky}=3.5$ is simulated for two different initial lateral deviations ($y_0 = 0.05$ and $y_0 = 0.5$). Regardless of the initial conditions both curves converge to zero for this value of **c**. There is a unique stable steady state solution for this value of **c**. Figure (32) is simulated for $K < 0$ and $\omega_n = 0.4$ and the same initial condition of $y_0=0.5$. When $c = 3.5$ the simulation converges to zero as explained in Figure (31). When c is increased above the critical value (here $c=4.0$) we observe that the solution converges to a limit cycle. This stable limit cycle coexists with the unstable equilibrium solution.

Figures (33) and (34) are presented to show the effects of a subcritical Hopf bifurcation. For this purpose $\omega_n=1.2$ is simulated for Figures (33), and (34). $\omega_n=1.2$ is in the region where $K>0$ in Figure (20). The initial condition for this case is

y_0= 0.05. When c is set to 3.5 the solution converges to zero, but for the case where c is set to 4.0 the simulations converge to a stable limit cycle. This is the case in Figure (11-b). The simulation misses the unstable limit cycles and converges to the outer limit cycle shown in Figure (11-b). In Figure (34) the effects of the initial conditions are further illustrated. In Figure (34) for y_0=0.05, the simulations converge to zero, but for y_0=0.5 the simulations converge to a limit cycle. For this simulation the initial condition was large enough to shift the results to a limit cycle rather than the zero steady state solution.

From the simulations we observe that in subcritical bifurcations the magnitude of the stable limit cycle is greater than the magnitude of the limit cycle in supercritical bifurcations. Similar results can be obtained for the other cases of variation in parameters a, b, and gains K_ψ and K_y .

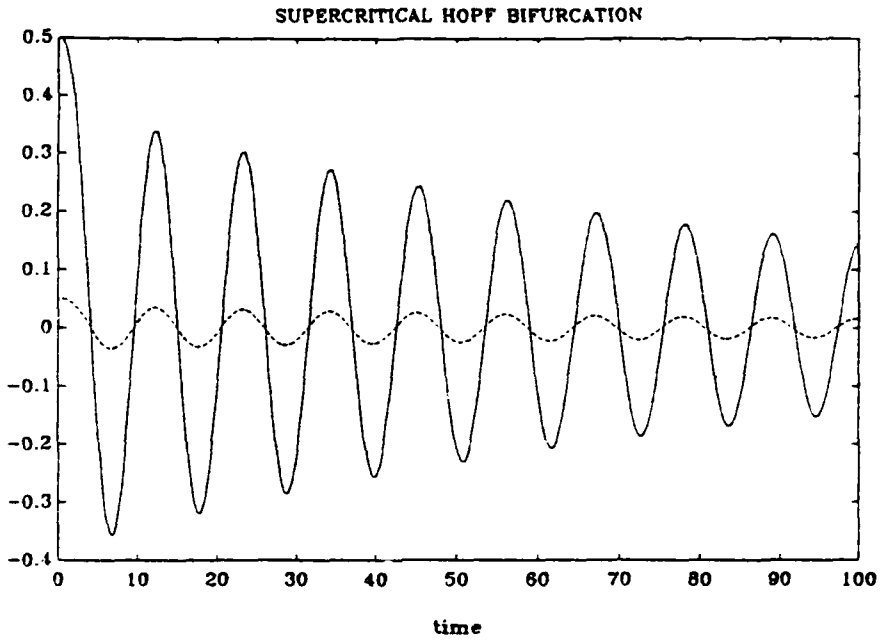

Figure 31 Supercritical Hopf bifurcation for $\omega_n=0.4$, $c=3.5$ for two simulations with $y_0=0.05$ and $y_0=0.5$.

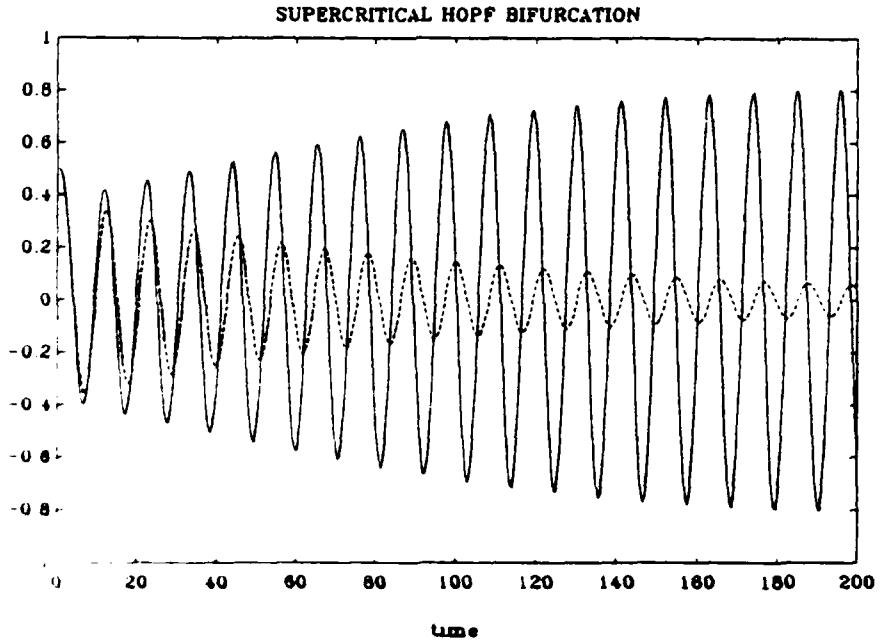

Figure 32 Supercritical Hopf bifurcation for $\omega_n=0.4$, $y_0=0.5$ for two simulations $c=3.5$ (stable equilibrium) and $c=4$ (unstable equilibrium) .

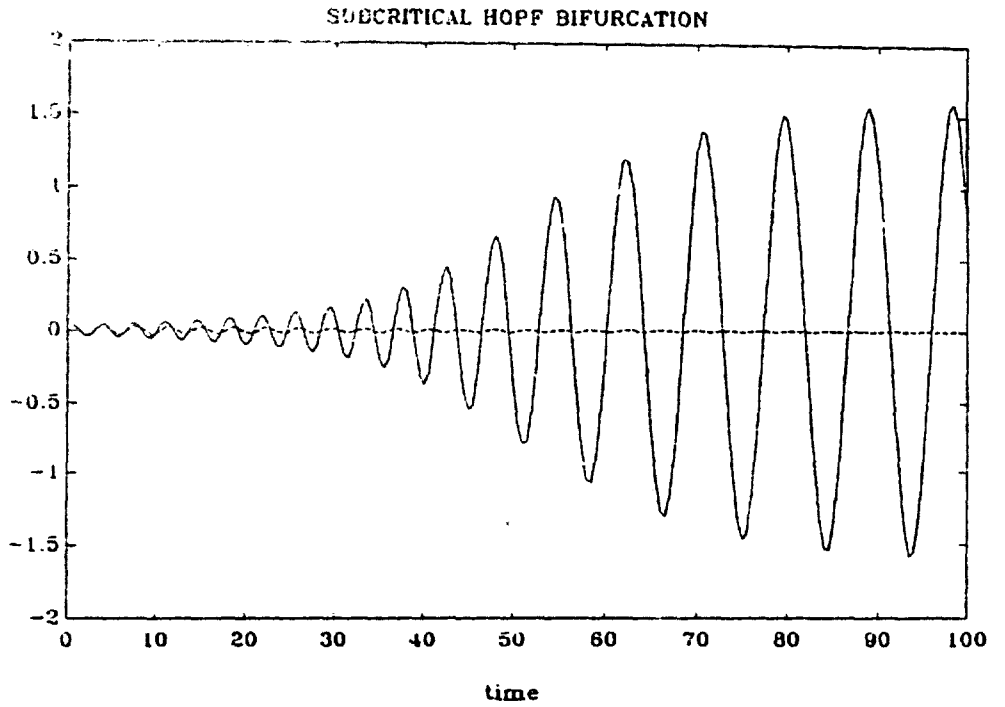

Figure 33 Subcritical Hopf bifurcation for $\omega_n=1.2$, $y_0=0.5$ for two simulations c=3.5 (stable equilibrium) and c=4 (unstable equilibrium) .

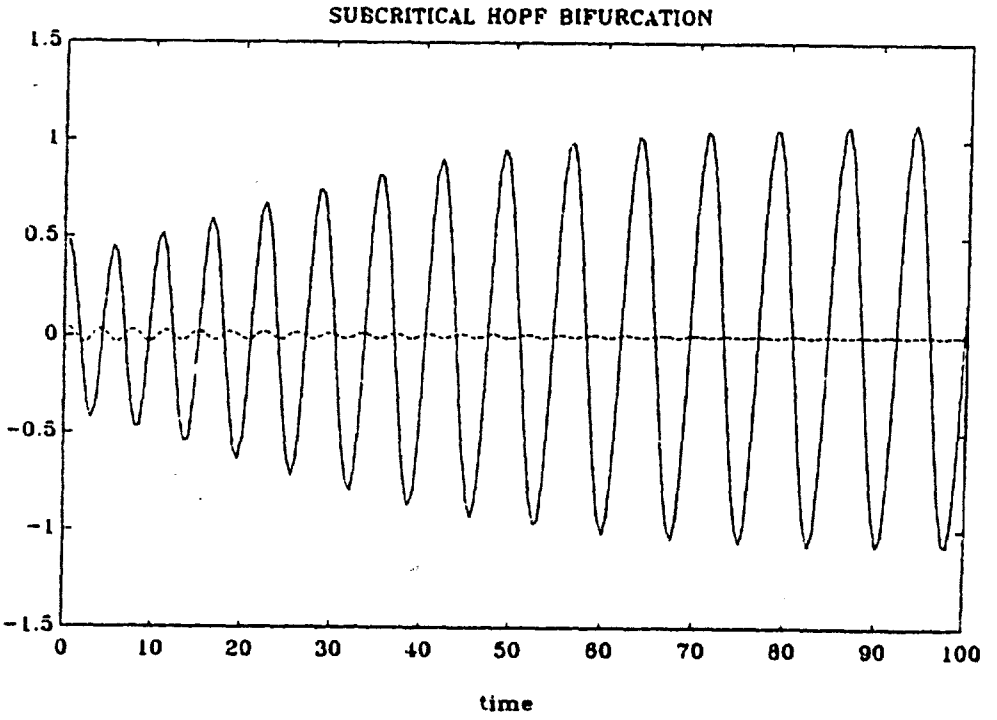

Figure 34 Subcritical Hopf bifurcation for $\omega_n=1.2$ (K>0) where c=3.5. The simulations for $y_0=0.05$ converged to the steady state value and for $y_0=0.5$ to the limit cycle.

V. SUMMARY AND CONCLUSIONS

An analytic investigation of the nonlinear dynamic response characteristics of a steering control law of marine vehicles has been presented. Bifurcation theory techniques were utilized in order to assess the behavior of the system upon initial loss of stability. The main bifurcation parameters were the natural frequency, control saturation level, system parameters and gains. The main conclusions of this research can be summarized as follows:

1. There exists a critical point for each gain and system parameters for stability of straight line motion. The loss of stability occurs in the form of Hopf bifurcation for each case. As the parameter crosses its critical value, a family of periodic orbits ("self oscillations") develops.

2. The desired characteristic equation from the ITAE criterion has a faster response for higher natural frequency. However, subcritical Hopf bifurcation develops when the natural frequency is sufficiently high. If **c** is increased past $\mathbf{c}_{crit}$ the amplitude of lateral deviation undergoes a jump and takes "large" values ("hard loss of stability or hard generation of limit cycles"). For lower natural frequencies, stability loss occurs as supercritical where the limit cycle amplitude grows continuously (" soft loss of stability").

3. The stationary point where change of stability occurs is related only to the natural frequency of the system and the hydrodynamic coefficient **a**.

4. Higher saturation limit of the rudder angle increases the range for supercritical Hopf bifurcation. Theoretically, if a saturation limit does not exist all bifurcations develop as supercritical.

5. The term a_3 has a similar effect as the saturation limit of rudder angle. An increase in the $|a_3|$ term increases the natural frequency where supercritical Hopf bifurcation exists, but an increase in the $|a_3|$ term is not a desired condition since vehicle response to rudder angle slows down.

6. Transitions from supercritical to subcritical are very important for the design of the control law. A supercritical Hopf bifurcation is preferred over a subcritical Hopf bifurcation since the subcritical Hopf bifurcation may develop a rapid dynamic jump to a new limit cycle.

Some recommendations for further research are as follows:

1. Comparative studies must be performed including the observer dynamics. The effect of variations in gains and system parameters must be studied to predict the accuracy of the observer.

2. Continuation techniques for periodic solutions must be performed for further stability analysis. The cases for simultaneous variations of more than one terms must be studied to understand the dynamic response of the system including any nonlinear terms.

LIST OF REFERENCES

Bahrke,K. *On-line Identification of the Steering and Diving Response Parameters of an Autonomous Underwater Vehicle from Experimental Data*, Mechanical Engineer's Thesis. Naval Postgraduate School, Monterey, California, 1992.

Chow, S. N. and Mallet-Paret, J. "Integral Averaging and Bifurcation," *Journal of Differential Equations*, Vol. 26, pp. 112-159, 1977.

Crane, C. L., Eda, H., and Landsburg, A., *Principles of Naval Architecture (ed. E. V. Lewis)*, The Society of Naval Architects and Marine Engineers, New York, 1989.

Friedland, B., *Control System Design; An Introduction to State Space Methods*, Mc-Graw Hill, New York, 1986.

Guckenheimer, J. and Holmes P., *Nonlinear Oscillations, Dynamical Systems, and Bifurcations of Vector Fields. Applied Mathematical Sciences 42*, Springer-Verlag, New York, 1983.

Hassard, B. and Wan, Y.H., "Bifurcation Formulae Derived from Center Manifold Theory," *Journal of Mathematical Analysis and Applications*, Vol. 63, pp. 297-312, 1978.

Healey, A. J., "Model-based Maneuvering Controls for Autonomous Underwater Vehicles," *Journal of Dynamic Systems, Measurement, and Control, Transactions of the ASME*, Vol. 114, pp. 614-622, 1992.

Papoulias, F. A. and Healey, A. J., "Path Control of Surface Ships Using Sliding Modes," *Journal of Ship Research*, Vol. 36, p. 2, 1992.

Papoulias, F. A., "Bifurcation Analysis of Line of Sight Vehicle Guidance Using Sliding Modes," *International Journal of Bifurcation and Chaos*, Vol. 1, p. 4, 1991.

Parsons, M. G. and Cuong, H. T., *Optimal Stochastic Path Control of Ships in Shallow Water*, Office of Naval Research Report No. ONR-CR-215-249-2F, 1977.

Parsons, M. G. and Cuong, H. T., *Adaptive Path Control of Surface Ships in Restricted Waters*, Department of Naval Architecture and Marine Engineering, Report No. 211, The University of Michigan, Ann Arbor, 1980.

Parsons, M. G. and Cuong, H. T., *Surface Ship Path Control of Surface Ships in Restricted Waters*, Department of Naval Architecture and Marine Engineering, Report No. 233, The University of Michigan, Ann Arbor, 1980.

Yoerger, D. R. and Slotine, J. J., "Robust Trajectory Control of Underwater Vehicles," *IEEE Journal of Oceanic Engineering*, Vol. 10, p. 4, 1985.

Seydel, R., *From Equilibrium To Chaos*, Elsevier, New York, 1986.

Papoulias, F. A., "On the Nonlinear Dynamics of Pursuit Guidance For Marine Vehicles," submitted for publication to Journal of Ship Research, 1992.

Carr, J., *Applications of CENTER Manifold Theory*, *Applied Mathematical Sciences 35*, Springer-Verlag, New York, 1981.

Marsen, J. E. and Mc Cracken M., *The Hopf Bifurcation and Its Applications*,. *Applied Mathematical Sciences 19*, Springer-Verlag, New York, 1976.

Thompson, J. M. T. and Stewart, H. B., *Nonlinear Dynamics And Chaos*, John Wiley and Sons, New York, 1986.

Dorf, R. C., *Modern Control Systems*, Addison-Wesley Publishing Company, 1992.

INITIAL DISTRIBUTION LIST

		No. Copies
1.	Defense Technical Information Center Cameron Station Alexandria VA 22304-6145	2
2.	Library, Code 052 Naval Postgraduate School Monterey CA 93943-5002	2
3.	Chairman, Code ME Department of Mechanical Enginnering Naval Postgraduate School Monterey CA 93943-5000	1
4.	Professor Fotis A. Papoulias, Code ME/PA Department of Mechanical Engineering Naval Postgraduate School Monterey CA 93943-5000	3
5.	Deniz Kuvvetleri Komutanligi Personel Daire Baskanligi Bakanliklar, Ankara/TURKEY	2
6.	Golcuk Tersanesi Komutanligi Golcuk, Kocaeli/TURKEY	1
7	Deniz Harp Okulu Komutanligi 81704 Tuzla, Istanbul/TURKEY	1
8	Taskizak Tersanesi Komutanligi Kasimpasa, Istanbul/TURKEY	1
9.	Zeki O. Oral 6. Cadde 35/12 Bahcelievler, Ankara/TURKEY	1